Magnetic Nanoparticles for Biomedical Applications

15

Manuel Bañobre-López, Y. Piñeiro, M. Arturo López-Quintela, and José Rivas

Keywords

Magnetic hyperthermia • Magnetic nanoparticles • Magnetic resonance imaging • Particle surface functionalization

Introduction

Nanotechnology emerged as a powerful discipline able to synthesize and manipulate materials at the nanoscale. The chemical and physical properties of bulk materials were found to drastically change when the particle size was reduced to the nanometer scale, basically due to the big increase of the surface-to-volume ratio. The discovery of these remarkably unique size-dependent chemical and physical properties allowed the development of new research areas that have led to important results in both fundamental and applied sciences. Most of these achievements have changed the way in which our society behaves nowadays. Even at the nanoscale, different materials structures can be found attending to their dimensionality (Fig. 15.1). In this chapter, we will focus on the applicability of magnetic nanoparticles, which are considered 3D materials with enhanced surface-to-volume ratio.

If within the vast world of nanotechnology we need to highlight one topic that resulted to be an authentic revolution in several areas of knowledge, this is the use of magnetic nanoparticles. During the last decades, magnetic nanoparticles have attracted much attention, since a big number of opportunities are

M. Bañobre-López (✉) • J. Rivas
International Iberian Nanotechnology Laboratory (INL), Braga, Portugal
e-mail: manuel.banobre@inl.int; jose.rivas@inl.int; jose.rivas@usc.es

Y. Piñeiro • M.A. López-Quintela
Departments of Physical Chemistry and Applied Physics, University of Santiago de Compostela, Santiago de Compostela, Spain
e-mail: y.pineiro.redondo@usc.es; malopez.quintela@usc.es

B. Bhushan et al. (eds.), *Handbook of Nanomaterials Properties*,
DOI 10.1007/978-3-642-31107-9_29,

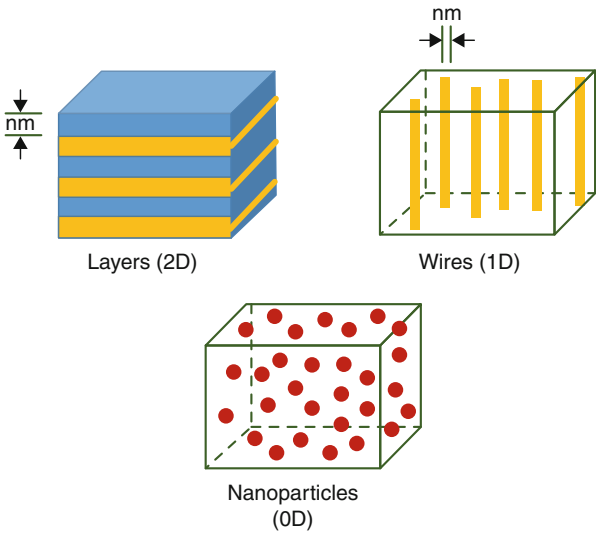

Fig. 15.1 Material structures depending on their dimensionality

opened when their size-tunable magnetic properties are combined with other size-dependent chemical or physical properties, i.e., optical, magnetoresistance, thermoelectric and biocide properties, and surface functionalization ability. Other research disciplines have noticed in the use of magnetic nanoparticles a novel and original solution to many of their problems. The collaboration of different areas of knowledge has been of fundamental importance for the development of advanced magnetic nanosystems. Such interdisciplinary motivated the design of multifunctional nanoparticles able to fulfill several chemical and physical requirements needed for a given application (Fig. 15.2). Nowadays, multifunctional particles play an important role in different technological areas with potential applications in fields such as electronics [1], energy [2], and biomedicine [3]. Its research involves the design, synthesis, and characterization of a wide variety of unconventional magnetic nanoparticles and core-shell nanostructures. Depending on their composition, particle size and distribution, morphology, structure, and different particle assemblies, magnetic nanoparticles have demonstrated a diverse range of useful bioapplications going from magnetic resonance imaging, magnetic separation, carriers for drug delivery to cell and tissue targeting or hyperthermia [4–6].

The use of magnetic nanoparticles in nanomedicine implies the use of biocompatible nanoparticles, so different functionalization strategies can be carried out to improve their biocompatible character, i.e., coating with organic or inorganic compounds. Within the biocompatible magnetic nanoparticles, superparamagnetic nanoparticles are especially interesting. At the nanometer scale, magnetic properties depend on the particle size. In a top-down approach, the reduction of the particle size is accompanied of an energetically favorable destruction of magnetic

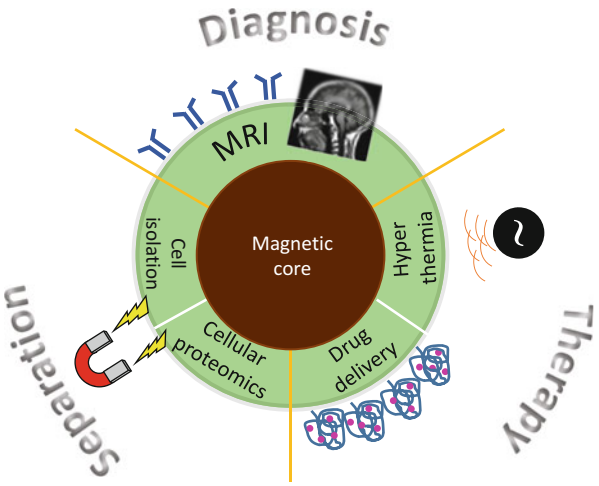

Fig. 15.2 Illustration of a multifunctional nanoparticle

domain walls, in such a way that below a certain particle size, the formation of only one single domain is favored. The magnetic behavior of these single-domain particles is known as superparamagnetism, and it is basically characterized by having no coercive forces or remanence, what means that they exhibit nule magnetization when the applied magnetic field is removed. And this is of great importance in biomedicine, since it avoids the magnetic dipolar interaction between nanoparticles and so their aggregation.

Along this chapter, we will briefly describe the main chemical routes widely used to prepare magnetic nanoparticles. Several modifications and new methods are continuously emerging with the aim of (i) controlling more precisely the properties of the magnetic nanoparticles and (ii) searching more environmental friendly and less cost-effective procedures. We will focus on the most established methods and those general aspects settle out as their basis. Then, we will discuss about the importance of the particle functionalization for biomedical applications and which are the main strategies carried out with this purpose. Next sections will focus on the most researched applications of magnetic nanoparticles in the biomedical field, describing the basic principles of the techniques involved and reviewing the main related findings in those fields. Finally, a perspective with future considerations will be speculated.

Synthesis

The most used form of magnetic particles in nano-biomedicine is as aqueous colloidal dispersions. The colloidal stability depends strongly on the particle size and surface functionalization, so they should be sufficiently small to avoid the natural gravitation forces and preferentially show significant

electrostatic/steric particle interactions [7]. Inorganic nanometer-sized colloidal dispersions have been extensively used in many biomedical applications due to their contrasted good optical, electronic, and magnetic properties, which are dependent on their composition, particle size, and morphology [8, 9]. In order to guarantee reproducibility and high-quality performance, monodisperse nanoparticles in both size and shape are highly demanded. The synthesis is the most powerful tool to act over these parameters, and it will determine the particle size and distribution, morphology, surface activity, and, therefore, their chemical and physical properties. There are a lot of critical parameters involved in a chemical reaction that eventually will origin the desired product. Starting precursors, ion concentration, temperature, time, and atmosphere are only some of them, and depending on how much precisely we will control them we will have better or worse control in the final structure and related properties. The use of templates is also widely used for the synthesis of some materials with specific structures and properties. Some of them are used as nanoreactors in which the particle size can be controlled or limited by physical constrains, as in the case of microemulsions. Several functional materials can be also used as building blocks to form more complex systems that integrate different properties, as, for example, bimetallic alloy particles or core-shell structures [10].

Following, we will describe the most established methods for the synthesis of improved uniform magnetic nanoparticles, essentially involving solution techniques. We will mainly focus on those methods that can be used to obtain iron oxide nanoparticles, since due to their chemical stability, their well-known size-tunable physical properties, surface chemistry, and biocompatibility, they are the most accepted candidate materials for in vivo applications.

Coprecipitation

Coprecipitation is the most popular method to synthesize iron oxide nanoparticles in a facile, fast, and scalable way. Either Fe_3O_4 (magnetite) or γ-Fe_2O_3 (maghemite) can be obtained from an aqueous solution containing Fe^{2+} and Fe^{3+} ions by addition of a base under inert atmosphere at room temperature or higher. There are several parameters that determine the final particle size, shape, and surface charge of the nanoparticles, such as the Fe^{2+}/Fe^{3+} salt precursors (nitrates, chorides, sulfates), the Fe^{2+}/Fe^{3+} ratio, pH, temperature, and ionic strength of the media. It is important to mention that magnetite nanoparticles are not very stable under ambient conditions and are easily oxidized to maghemite. However, from the magnetic point of view this is not a serious problem since maghemite is also a ferrimagnet with similar high saturation magnetization. The synthesis of magnetite nanoparticles with a controllable particle size and narrow distribution is highly desired for both in vivo (i.e., MRI, hyperthermia, drug delivery) and in vitro (i.e., biosensing, magnetic separation) biomedical applications.

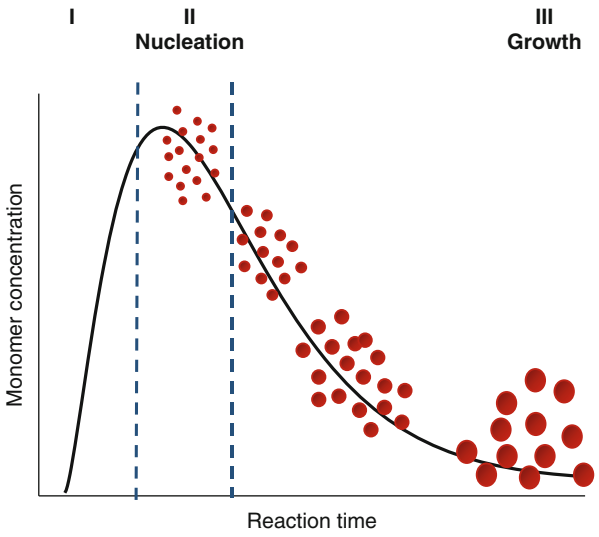

Fig. 15.3 Classical model of LaMer and Dinegar for the mechanism of formation of uniform particles in solution

And, unfortunately, general coprecipitation methods lead to polydisperse nanoparticles. Due to the size-dependent magnetic properties, a broad particle size distribution will result in a wide range of blocking temperatures and, therefore, in a non-optimized magnetic behavior for those applications in which deviations from a superparamagnetic behavior are not recommended. In a general homogeneous precipitation a short burst of nucleation occurs when the concentration of constituent species reaches the supersaturation. Then, these nuclei grow uniformly to give rise to bigger nanoparticles [11] (Fig. 15.3). It is well known that the final particle monodispersity will depend on how these two processes develop. An efficient separation of the nucleation and nuclei growth stages, as well as a slow growth process, is needed to achieve high monodisperse nanoparticles.

However, other mechanisms involving simultaneous nucleation events and *Ostwald ripening* growth (continuous growth by diffusion) [12] and smaller particle *aggregation* [13, 14] have been also proposed to explain the formation of monodisperse nanoparticles. Other coprecipitation methods have been developed to achieve homogenous and monodisperse magnetite nanoparticles, i.e., from aqueous ferrous and ferric hydroxides by aggregation of the initial small particles originated in the hydroxide gel (*seed*-based methods).

The use of different organic coatings and additives has been a useful tool to increase the monodispersity of the magnetite/maghemite nanoparticles and also their biocompatibility, making them interesting for in vivo applications. Among a long list of stabilization agents, oleic acid (OA) [15, 16], polyacrylic acid (PAA) [17], polyethylene glycol (PEG) [18], polyvinyl alcohol (PVA) [19], polyvinylpyrrolidone (PVP) [20], polysaccharides [21, 22], and other synthetic polymers have been some of the most successfully used. It is important to

mention that all these coating agents or stabilizers can greatly affect the atomic structure at the particle surface and so preserve the spin alignment observed in the inner core [23].

Thermal Decomposition

The thermal decomposition of iron precursors at relatively high temperatures and in presence of appropriate surfactants improves significantly the crystallinity of iron oxide nanoparticles and leads to a better size and shape controlled particles with narrow size distributions. Basically, monodisperse magnetic nanocrystals between 4 and 20 nm can be synthesized through the thermal decomposition of organometallic compounds in high-boiling organic solvents containing stabilizing surfactants [9]. In the particular case of magnetite/maghemite nanoparticles, the commonest used organometallic precursors are iron pentacarbonyl [$Fe(CO)_5$], iron tri-acetylacetonate [$Fe(acac)_3$], and $FeCup_3$ (Cup: *N*-nitrosophenylhydroxylamine). Whereas in the first case (Fe in 0 valence) the reaction goes through the intermediate metal formation, that will be later on oxidized to magnetite by addition of a mild oxidant (trimethylamine oxide) [24], the synthesis using the $Fe(acac)_3$ as starting material leads directly to the maghemite nanoparticles [25, 26]. Maghemite nanocrystals between 4 and 10 nm were obtained by injection of FeCup3 solutions in octylamine into long-chain amines at 250–300 °C in octylamine.

In general, fatty acids, oleic acid, oleylamine, and hexadecylamine are commonly used as surfactants, whereas the use of a specific solvent depends on the solubility of the other reagents and the maximum temperature that will be raised during the reaction. Some representative examples of solvents used in this method are octylamine, phenyl ether, phenol ether, octyl ether, hexadecanediol, octadecene, 1-hexadecene, and 1-octadecene, among others, and the main characteristic of most of them is their high boiling temperature. For example, magnetite nanoparticles with sizes from 3 to 20 nm have been synthesized reaction of $Fe(acac)_3$ in phenyl ether in the presence of alcohol, oleic acid, and oleylamine at 265 °C [26]. It is especially interesting to mention a different approach developed by Park et al. [27], in which they use iron chloride [$Fe(Cl)_3$] and sodium oleate to generate an intermediate iron oleate complex that is later on decomposed at high temperatures between 240 °C and 320 °C.

However, all these experimental procedures lead to magnetic nanoparticles dispersible in organic solvents such as toluene or hexane. Different particle surface modification strategies have been developed to transfer after synthesis these organic-stabilized nanoparticles to aqueous solvents. For example, water-soluble magnetite nanoparticles have been directly prepared by thermal decomposition of $FeCl_3 \cdot 6H_2O$ and 2-pyrrolidone under reflux at 245 °C and also in similar conditions by addition of carboxyl-terminated poly(ethylene glycol) as coating agent [28, 29].

Although we have focused mainly on the synthesis of magnetite, thermal decomposition procedures in which metal-organic precursors are boiled at high temperatures in organic solvents can be extended to the synthesis of other metal

transition oxides (Fe, Mn, Co, Ni, Cr), metallic nanoparticles (Fe, Ni, Co), or alloys ($CoPt_3$, FePt) which could be also useful for specific biomedical applications [9]. Moreover, thermal decomposition has settled out as one of the best methods to prepare magnetic nanoparticles with a good control of the particle size and morphology.

Microemulsions

Everybody has experienced at some point the phenomenon that arises when two immiscible solvents are mixed (i.e., water and oil). However, the addition of a surfactant can stabilize the dispersion of one of the phases in the other. Surfactants are amphiphilic molecules with two well-differentiated parts: one hydrophobic and other hydrophilic. They are placed in the interface between the aqueous and the organic phases reducing the surface tension between them and allowing the stable dispersion of one phase within the other through the formation of different structures, such as small drops, cylinders, and layers, depending on the mass relation between the aqueous and organic phases and surfactant. Therefore, a *microemulsion* can be defined as a thermodynamically stable isotropic dispersion of two immiscible liquids where the microstructures are stabilized by an interfacial layer of surfactant molecules.

The *microemulsion* technique is a powerful method to prepare simple metallic and oxide NPs, as well as, core-shell and 'onion-like' NPs [30–32]. Although microemulsions cannot be considered as real templates, they constitute an elegant technique that provides a very good control of the final particle size. The reason for that is a complex interplay mainly between three parameters, namely, surfactant film flexibility, reactant concentration, and reactant exchange rate [33]. By adequately choosing these three parameters, one can get a homogeneous distribution of particle sizes down to few atoms. In the particular case of microemulsions, the diameter of the microdroplets typically ranges from 1 to 50 nm. The main physical properties of microemulsions are transparency (the structures are so small that there is no light dispersion), low viscosity, and high stability that avoid the phase separation with time. Depending on what phase is dispersed, microemulsions can be classified as water-in-oil (W/O) or oil-in-water (O/W) when the oil is dispersed in the aqueous phase. The most used in the synthesis of magnetic nanoparticles is the case of water-in-oil microemulsions, because it allows the aqueous microdroplets to behave as nanoreactors in which the reaction takes place. The size confinement created inside these cavities limits the particle nucleation, growth, and agglomeration.

In a typical procedure, nanoparticles will be obtained by mixing two identical W/O microemulsions containing the desired reactants dissolved in the aqueous phase inside the droplets, one of them with the metal ions of interest and the other with the reducing agent. The method is based on continuous collisions between microemulsions, followed by their coalescence and reactants exchange, that will start the reaction and eventually will give place to the formation of

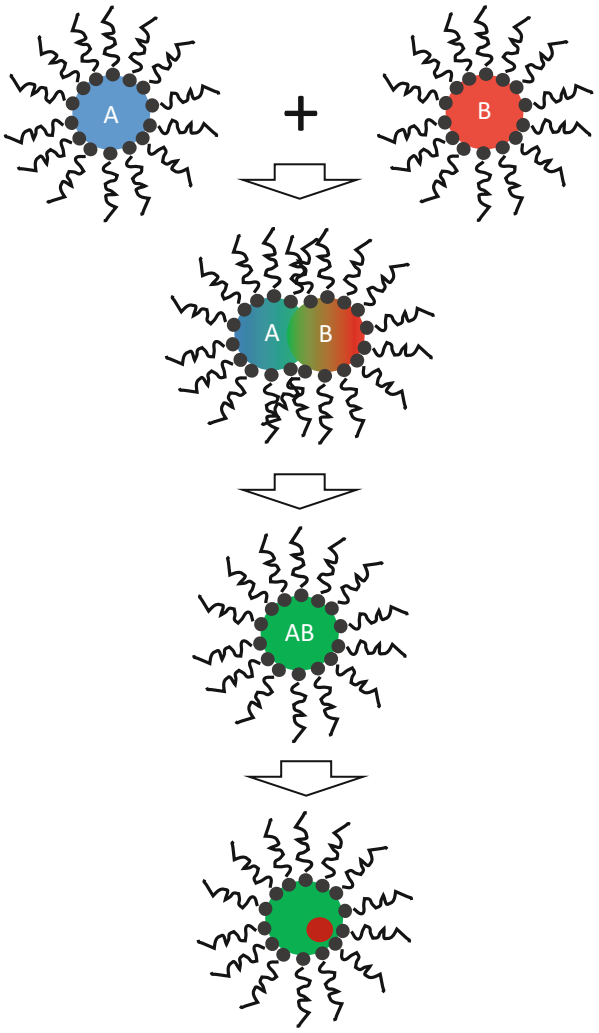

Fig. 15.4 Schematic representation of a microemulsion reaction

a precipitate inside the reverse micelles (Fig. 15.4). This precipitate can be extracted by adding acetone or ethanol, which breaks the droplets integrity, and then filtering or centrifuging the original mixture. The normal particle sizes that can be obtained by this method are below 20 nm and they can be controlled by the volume ratio of water to the organic solvent and amount of surfactant used. Some representative examples of microemulsion systems for the particular synthesis of magnetite can be found in the literature. For example, $FeCl_2$ and $FeCl_3$ chlorides can be hydrolyzed with ammonium hydroxide inside spherical drops of water-in-oil generated by AOT as surfactant in heptane as continuous phase to obtain magnetite nanoparticles of 4 nm [30]. Other similar microemulsions can be formed by using different surfactants (CTAB, SDS,

dodecylbenzenesulfonate (NaDBS)) and oil phases (octane, toluene, heptane, etc.). Also core-shell structures [34] and different particle shapes droplets [35] can be obtained through this method by an appropriate design of the dispersed reverse micelles [36, 37].

Although the microemulsion method is useful to synthesize monodispersed nanoparticles with different morphologies, the large volume of solvent that it needs, its low yield in comparison to the coprecipitation or thermal decomposition methods and the difficulty for an industrial scale-up are some of its main disadvantages.

Hydrothermal

The hydrothermal method is based on a solid-liquid-solution reaction in which a phase transfer and separation process occur at the solid-liquid and solid-solution interfaces along the reaction time. This method was reported by Li et al. [38], who synthesized high crystalline and water-soluble magnetite and ferrites by using $FeCl_3$ as iron source, ethylene glycol as high-boiling solvent and reducing agent, and sodium acetate and polyethylene glycol as electrostatic and steric stabilizers, respectively, to avoid the particle aggregation [39]. In a typical experiment, this multicomponent reaction mixture would be stirred and sealed in a teflon stainless autoclave that will be later heated up at temperatures around 200 °C for times up to 72 h. Depending on the reaction temperature and duration, the particle size and distribution would be modified. Although this method has been only a little explored for the synthesis of magnetic nanoparticles, it leads to high-quality structural and morphological particles.

Other solution-based techniques also used in the preparation of magnetic nanoparticles for biomedical applications are the *polyol* process, *pyrolysis*-related methods (laser and spray), *aerosol*/*vapor* methods, *sonochemical-assisted* methods, and *electrochemical* methods, in which the particle size can be tuned by applying a different current density [40].

Functionalization

Applications of magnetic nanoparticles in life sciences fields, such as biotechnology and biomedicine (diagnosis and therapy), imply the use of stable colloidal dispersions in which the nanoparticles are dispersed in different liquid mediums, i.e., blood, urine, physiologic and medium. The colloidal stability of these fluids depends mainly on two parameters: first, on the dimensions of the particles, which should be small enough to avoid their precipitation due to the gravitation forces and, second, on the charge and surface chemistry that determine the steric and coulombic repulsions [7]. All the magnetic nanoparticles used in biomedicine concerning in vivo applications must be properly coated or functionalized for several reasons: an adequate coating of the particle surface not only provides better

stability to the colloidal dispersions avoiding the formation of large aggregates but also prevents structural changes and biodegradation (i.e., oxidation, biological pH changes) that could irreversibly deteriorate their physicochemical properties when exposed to real physiological systems.

On other hand, one of the most important issues for the successful and efficient performance of magnetic nanoparticle-based systems in biomedical applications depends greatly on our ability to drive them to the area of interest, so a proper surface modification should allow attaching ligands for specific target recognition of the desired species (molecules, cells, tissues, or organs). There are several strategies of surface functionalization involving different coating agents that help us to get this goal. Among them, we can mention polymers, virus, antibodies (that recognize specifically proteins), aptamers (show high affinity to certain molecules), etc. Also many polymers and hydrogels have been widely used as coating agents of nanoparticles that allow binding drugs by covalent attachment, adsorption, or entrapment on the particle surface [41] and which will be released precisely in the area of interest under certain chemical or physical stimuli, either internally or externally induced (i.e., internal physiologic pH change or an application of an oscillating magnetic field for hyperthermia, respectively). In the particular case of magnetic nanoparticles, one of the most desirable administrations via would be by intravenous injection, so the additional creation of strong enough magnetic forces by permanent magnets could guide them to the target tissue, overcoming the blood flow forces naturally generated in the blood circulation system.

Additionally to the reasons described above, a suitable particle surface modification or coating is also a useful tool to improve their biocompatibility and nontoxicity, avoiding as much as possible the activation of the immune system agents. Attending only to considerations purely related to physical properties, there would be several materials with better magnetic specifications than iron oxides and which would show a better performance for many of the biomedical applications that have been mentioned here. However, the toxicity associated to these materials constitutes an important drawback. In a big extent, this toxicity is determined by the nature of the magnetic core. Magnetic materials with very good magnetic performance, such as Co or Ni, are considered non-useful for biomedical applications due to their proved toxicity [42, 43]. For this reason, the commonest materials used in biological applications are mostly iron oxides, such as magnetite, maghemite, and other ferrites, for which several protocols of particle surface functionalization have been already established for various biomedical applications [44].

Several multifunctional structures have been designed to improve the colloidal stability and the biocompatibility of magnetic nanoparticles for applications in biomedicine. Among them, we can emphasize core-shell nanostructures [10], in which the external layer does not only preserve the chemical and physical properties of the core against oxidation by oxygen or erosion by acids or bases but also increase the time stability avoiding agglomeration or precipitation and provides the nanoparticle with a more feasible surface to be further functionalized with organic and inorganic functional molecules and compounds. Coatings with organic shells involve polymers and surfactants, such as fatty acids or phospholipids [45–50],

whereas inorganic coatings include silica [51, 52], precious metals [53], or oxides [54]. In the case of ferrofluids the particle size and the surface properties are the main factors that determine the colloidal stability, so electrostatic or steric repulsions are often used to achieve highly stable colloidal dispersions. Surfactants and polymers can be chemically anchored or physically adsorbed to the nanoparticle surface to form single or double layers [55] that balance the attractive dipolar magnetic interactions and the van der Waals forces, which tend to aggregate magnetic nanoparticles in solution. Among others, some of the polymers having functional groups (carboxylic acids, phosphates, sulfates, etc.) that allow them to bind to the particle surface are poly(aniline), poly(pyrrol), poly(glycolic acid), poly (lactic acid), poly(ε-caprolactone), etc [56]. Some representative examples of stabilizations with polymers and surfactants involving iron oxides are peptizations of magnetite nanoparticles with tetramethylammonium hydroxide (TMAOH) [57], coatings with poly(aniline) in the presence of the oxidant ammonium peroxodisulfate [58], polystyrene coatings of ferrites nanoparticles [59], or coatings with poly(acrylic acid) shells [17]. The synthesis methods described in the literature to fabricate these stable core-shell structures is diverse, from coprecipitation and microemulsion methods [60] to oxidative polymerizations [58] or atom transfer radical polymerizations [59].

Regarding inorganic coatings, gold and silica protective shells are two of the most extensive researched coatings for biomedical applications. Gold shells have been mostly used to coat metallic iron nanoparticles [53], whereas silica coatings have been successfully applied also to iron oxides [9, 61]. Both gold and silica coatings have several advantages since they provide nanoparticles with an enhanced stability in aqueous solvents, they have an easy surface modification, and can control the interparticle interactions by variation of the shell thickness. Moreover, their low reactivity and its very well-known surface chemistry allow to introduce further functionalization and additional functionalities, what makes them very promising for targeting drug delivery, bio-labeling, and tissue or molecular imaging. Regarding their synthesis, the method commonly used for gold coatings imply the use of wet chemistry procedures in which $HClAu_4$ is used as starting material to coat iron nanoparticles previously reduced in microemulsions formed by CTAB as surfactant, 1-butanol as cosurfactant, and octane as continuous oil phase [53]. Also a coating of Au on the surface of Fe_3O_4 nanoparticles has been achieved by reducing $HAuCl_4$ in a chloroform solution of oleylamine [62]. In the case of silica coatings, the commonest experimental procedures to coat iron oxides nanoparticles involve the Stöber method and sol-gel processes [63, 64] which basically consist on a basic hydrolysis of tetramethyloxilane (TEOS) in aqueous solution at room temperature. The reaction between the oxide surface and silica takes place through the OH groups. By controlling the amount of TEOS added stepwise, the silica shell thickness can be modified [52]. Sometimes, the natural formation of a controlled oxidized shell under ambient conditions is a strategy to passive the particle surface and avoid further oxidization of the magnetic core. This is the case of iron nanoparticles that are oxidized under ambient conditions at room temperature to form core-shell iron/iron oxide nanoparticles [54]. The additional use of excess stabilizers provide core-shell

structures with extra chemical stability that preserves the high magnetic performance of the iron cores without increasing the cytotoxicity, making them useful for cellular MRI applications. In both organic and inorganic coatings, the protective shells allow further surface modifications, such as the addition of specific targeting ligands, dyes, or therapeutic agents, that make them suitable for MRI, hyperthermia-targeted therapies, drug delivery vectors, etc.

Moreover, the coating material determines in a great extent the biodistribution and the half-life of the magnetic nanoparticles in the blood circulation system without being phagocyted by cells belonging to the reticuloendothelial immune system. The surface charge also plays an important role in blood half-lives, being the neutral ones those recommended to extend circulation times. The development of longer circulating MNPs has allowed the imaging of particular pathologies, such as tumors and inflammatory and infectious issues.

An appropriate surface modification also provides active sites for subsequent functional conjugation with biological or chemical functional moieties [65–67]. Although we will not focus on specific biological functionalizations, since there is a considerable amount of them depending on the specific targeting and application, we would like to mention some of the commonest surface modification strategies to activate the reactivity of the particle surface for further targeted bioconjugation. As explained previously, iron oxides are the most used nanomaterials for biomedical applications because they are biocompatible and nontoxic and because they can be easily synthesized through coprecipitation of the Fe^{2+} and Fe^{3+} salts in basic medium. However, this method shows some drawbacks, such as the difficulty to obtain monodisperse particle size distributions. To solve this problem, other alternative methods have been successfully applied to obtain monodisperse iron oxide nanoparticles. The use of microemulsions as nanoreactors [68] and also organic chemical routes in which the nucleation of the nanoparticles takes place in organic solvents at high temperature [69] have been both the most successfully applied. However, nanoparticles synthesized in this way are normally stabilized by oleic acid and oleylamine and are strongly hydrophobic, so the most primary strategy to turn them into water-soluble colloidal dispersions useful for biomedical applications must be by surfactant addition or surfactant exchange. The former one consists in the addition of amphiphilic molecules containing both hydrophobic and hydrophilic moieties, in such a way that the hydrocarbon chain can form a bilayer with the hydrophobic component of the original one and the hydrophilic groups will be exposed to outside of the nanoparticles, rendering water soluble. On other hand, the ligand exchange is based on a direct replacement of the original stabilizer molecules by other amphiphilic ligands due to their stronger affinity by the particle surface (via a strong chemical bond), in such a way that the polar groups allow the phase transfer of the magnetic nanoparticles to aqueous solvents. Similarly, several amphiphilic polymers can be used to transfer hydrophobic magnetic nanoparticles from organic solvents to aqueous solutions. In order to avoid cluster formation by grafting of previously prepared polymers chains, a different approach was developed by which a polymer brush is growth directly from the particle surface. This requires the presence of ligands

onto the particle surface that act as initiators and induce the polymerization process. These ligands are attached to the surface by replacing the original stabilizers (usually oleic acid or oleylamine) by ligand exchange. In the particular case of iron oxides M. Lattuada et al. [70] used capping agents having one or more reactive carboxylic acid groups (that easily interact with the Fe^{3+} present in the particle surface) and are the ones responsible to induce the polymerization. The most widely used polymerization technique is the atom transfer radical polymerization (ATRP) [71, 72]. Also ring opening polymerization (ROP) [73] have been used to coat magnetic nanoparticles with biodegradable polyesters. Furthermore, by an appropriate selection of ligands and polymers, we will be able to provide the particle surface with different functional groups, including carboxylic acids, thiols, amines, and carbonyl, that will allow the immobilization of various biological moieties, such as peptides, proteins, and oligonucleotides. Some examples are carboxyl acid- and amine-terminated polyethylene glycol (PEG) ligands that allow to transfer hydrophobic nanoparticles from an organic solvent to an aqueous media and also the bioconjugation of biomolecules onto magnetic nanoparticles, i.e., chromones (cromoglycates) for drug delivery [48, 74], through, for example, the EDC/NHS amidation chemistry. Also organosilanes (amino-, carboxylic acid-PEG terminated silanes), bifunctional molecules (2, 3-dimercaptosuccinic, DMSA), carboxylated phospholipids, and variety of carboxylates, phosphates, phosphonates, or other multidentate ligands improved the stability and biocompatibility of nanoparticles, as well as specificity to target through bioconjugation with peptides or antibodies [45, 75, 76].

The surface modification described above is a requirement for the application of magnetic nanoparticles in biomedicine, since stable and water-soluble colloidal dispersions are required. Additionally, another objective of this initial surface modification is to leave reactive functional groups for further specific functionalization and so tailoring nanosystems for a targeted application. As it would be impossible to cover all the biological functionalizations existent, we recommend to the reader the review of Schladt et al. and its references [61].

Biomedical Applications

With the increasing development of nanotechnology, more ambitious challenges are being searched with the aim to provide society with better efficient solutions. Most of the nanoparticle-based in vivo applications are very demanding and need the fulfillment of several requirements in order to guarantee their medical efficiency. Therefore, the integration of several functionalities in one single platform has become one of the most motivating issues in nanotechnology for biomedical applications. With this aim, the so-called *theranostic* nanoparticles emerged [77], referring to multifunctional nanoparticles with the ability to play important roles in both *diagnosis* and *therapy* applications. In this sense, magnetic nanoparticle cores and their appropriate surface functionalization provide nanoparticles with a very helpful multifunctional character in applications such

as cell and tissue targeting, bone tissue engineering, targeting drug delivery, magnetic separation, hyperthermia, and MRI. These complex nanostructured magnetic systems have enhanced the efficiency in therapeutics applications compared to conventional drugs, as well as reduce the harmful side effects [78], In some extent, this has been allowed due to a more localized targeting inside the desired area of the body, as well as to a longer time of residence in the body before being expulsed by the reticuloendothelial system and their ability to overcome specific biological barriers because of their small size, shape, and surface functionalization chemistry.

To cover all the biomedical applications of magnetic nanoparticles would be too much ambitious, so in this chapter the authors have decided to focus on, from our point of view, two of the most researched and projecting applications: magnetic resonance imaging and magnetic hyperthermia. We will try to explain to the reader the fundamentals of these techniques and interesting remarks about the research that is being carried out on them.

Magnetic Resonance Imaging (MRI)

Magnetic resonance imaging (MRI) is a powerful noninvasive medical radiology technique that uses the nuclear magnetic resonance (NMR) principle to visualize not only internal tissues and organs of the human body but also to monitor biological processes with high spatial resolution and without the use of ionizing radiation of radiotracers. MRI has become a very powerful technique in medical diagnosis, and now it constitutes one of the most researched topics in biomedicine, although still some limitations related to its imaging sensitivity need to be further improved. For these reasons, the ongoing research is focused on the search and development of new MRI contrast agents able to enhance the imaging resolution and so broaden the range of related applications.

MRI is based on the alignment and precession of the nuclear spins of protons around a strong applied magnetic field. Then, an extra transverse radio-frequency pulse (RF) is applied that disturbs these protons spins from the direction of the magnetic field and modify their relaxation time in their process to return to their original and more favorable lower-energy state. Two independent relaxation pathways can be monitored to generate an MR image: longitudinal relaxation (T1 recovery) that involves the recovering of the decreased net magnetization in the direction of the applied magnetic field and the transverse relaxation (T2 decay) that involves the disappearance of the induced magnetization in the perpendicular direction to the applied magnetic field, both as consequence of the energy transfer and spin dephasing after the application of the RF pulse, respectively (Fig. 15.5).

The contrast that can be appreciated in MR images is the result of local variations of the T1 and/or T2 relaxation times in adjacent regions. In other words, the spin-spin interaction between water protons nuclei and bio-macromolecules in biological tissues can induce variations in the local magnetic field that greatly affects the spin relaxation times of the nuclear spins of the

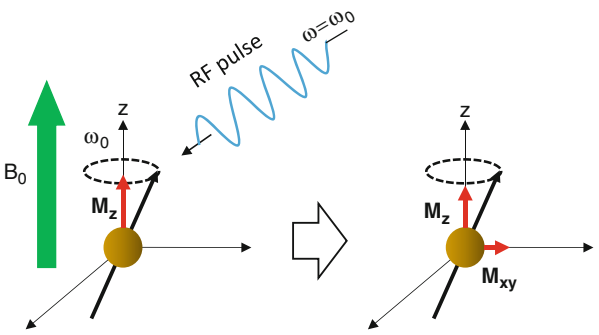

Fig. 15.5 Fundamentals of magnetic resonance imaging

surrounding hydrogen atoms. This spin dephasing can be caused by a combination of local inhomogeneities in the magnetic field due to tissue-inherent factors (intrinsic molecular interactions) or external sources (subtle variations in the external magnetic field) [79]. When the dephasing process accounts for both intrinsic molecular interactions and extrinsic magnetic field inhomogeneities, the images produced are called T2*:

$$\frac{1}{T_2{}^*} = \frac{1}{T_2} + \gamma Bs \tag{15.1}$$

where γBs represents the relaxation time caused by external field inhomogeneities. On the other hand, when the dephasing time accounts for the molecular interactions alone, it is called T2*-weighted (bright contrast).

MR contrast arises from proton density, as well as the chemical and physical nature of the tissues within the specimen. In most tissues, the variation of T1 and T2 between them is very small to observe good image contrast, so materials capable to enhance the contrast between the tissue of interest and the surrounding tissue are highly desired for clinical uses. These materials are called *contrast agents*, and depending over the relaxation process they act, they can be classified as T1 and T2 contrast agents, showing positive and negative contrast (bright and dark contrast, respectively). Currently, the most widely used clinical contrast agents are based on paramagnetic chelates of gadolinium [79, 80]. However, they present several drawbacks, such as short blood circulation times, poor detection sensitivity, and toxicity. These important issues resulted in the search of new and more efficient biocompatible contrast agents for MRI. In particular, those based on superparamagnetic iron oxides nanoparticles have been intensively developed in the last years due to their tunable physicochemical properties with size, shape, composition, and assembly, showing relatively high saturation magnetization, suitable surface chemistry, and biocompatibility [81]. When placed in an external magnetic field, each magnetic nanoparticle creates a local magnetic field that, in turn, induce local field inhomogeneities in the surrounding areas. In this scenario, when water molecules diffuse within the periphery of the MNPs, the coherent precessions of surrounding water proton spins are perturbed (Fig. 15.6). The net effect is a change

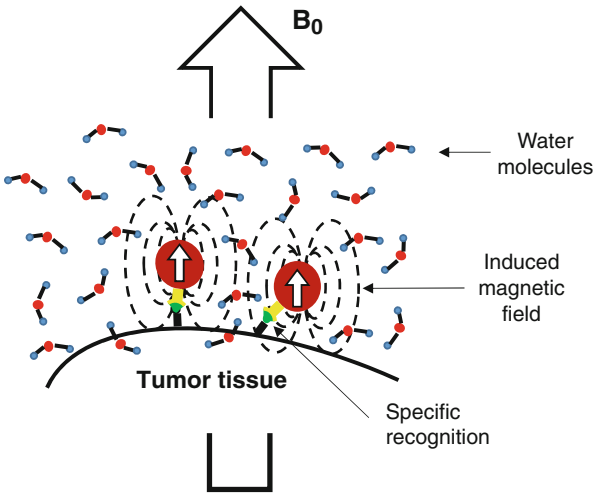

Fig. 15.6 Effect of MNP on the MRI contrast signal

in the magnetic resonance signal, which is measured as a shortening of the longitudinal (T1, spin-lattice) and transverse (T2, spin-spin) relaxation times, amplifying the signal difference between lesions and healthy tissues. For a T1 shortening a close interaction between protons and contrast agents is required, which can be hindered by the chemical nature and thickness of the coating agent around the MNP. On the other hand, the T2 shortening is caused by the large susceptibility difference between the particles and surrounding medium resulting in microscopic magnetic field gradients [82]. In particular, when superparamagnetic iron oxide-based nanoparticles present in tissues are subjected to an external magnetic field, the large magnetic moments of the particles align in the field direction, in such a way that create large field gradients through which water protons diffuse [83]. The dipolar coupling between the magnetic moments of water protons and the magnetic moments of particles causes efficient spin dephasing and T2 relaxation leading to a decrease in signal intensity (negative contrast) [84, 85].

For example, Bae et al. and Yang et al. synthesized T1/T2 dual contrast agents through modifying Gd-DTPA molecules on the surface of magnetic iron oxide nanoparticles [86, 87], and Choi et al. designed a core-shell nanostructure $MnFe_2O_4@SiO_2@Gd_2O(CO_3)_2$ in which the T1 and T2 contrast materials were magnetically decoupled and their relaxivities simultaneously maximized by adjusting the thickness of the silica shell in between them [88]. However, ultrasmall iron oxide NPs (Fe_3O_4/Fe_2O_3) continue to be better promising candidates due to their improved biocompatibility and stabilization in aqueous solutions [89, 90]. Additionally, they are especially interesting because of their high resistance to proteins adsorption and surface modification, which allow them to overcome some physiological barriers [91]. Nowadays, we can find several commercial brands using superparamagnetic iron oxide nanoparticles based on dextran or carbohydrate coatings, such as Ferridex, Combidex, Resovist, and

AMI-288/gerumoxytrol. More recently, FeCo NPs showed better MRI contrast than iron oxide NPs, although still some toxicity-related issues remain unsolved [92].

The efficiency of the contrast agents can be described by its longitudinal and transversal relaxivities, r1 and r2, respectively, which are the proportionality constant of the measured rate of relaxation, R1 (1/T1) and R2 (1/T2), over a range of contrast agent concentration. So, accumulation of MNPs in tissues in a significant concentration will enhance the MR contrast by shortening the relaxation of water surrounding protons. In general, the relaxivities are determined by three key aspects of the magnetic nanoparticles: [93].

(i) Chemical composition: It can greatly affect the contrast-enhanced capability of the nanoparticles, since ion defects and ion doping in specific sites of the structural lattice can result in a significant change of the magnetic structure and, therefore, also in a modification of the magnetic properties. By doping Fe_3O_4 with different cations at the octahedral sites, the resulting ferrites exhibit different relaxivities according to their different mass magnetization. For example, Mn-doped ferrite nanoparticles, $MnFe_2O_4$, show higher magnetic moment per unit and relaxivity values as high as 358 mM^{-1} s^{-1} at 1.5 T [15]. Further Zn doping in the tetrahedral sites resulted in even higher saturation magnetization and, consequently, in an enhanced relaxivity of 860 mM^{-1} s^{-1} at 4.7 T [94].

(ii) Particle size and degree of aggregation: transverse relaxivity is directly proportional to the magnetic moment of the particle. The saturation magnetization of magnetic nanoparticles is strongly dependent of the particle size and distribution, among other factors such as shape or surface modification, is increasing as the particle size increases. Therefore, the enhanced MR contrast induced by nanostructured magnetic materials is directly correlated with the particle size. The relationship between the transverse relaxivity (r2) and particle size was studied in uniform-sized iron oxide nanoparticles and was found to increase from 106 mM^{-1} s^{-1} to 218 mM^{-1} s^{-1} when the particle size increases from 6 to 12 nm [95]. Another different approach to increase the cross section of magnetic nanoparticles and enhance the MR contrast properties by shortening T2-weighted relaxation time is to fabricate magnetic nanoclusters consisting of smaller nanoparticles or embedded in polymeric matrixes [96, 97].

The shortening in the longitudinal relaxation time T1 is rather due to a direct magnetic interaction between the magnetic atoms in the particle surface and the surrounding protons. For this reason, the relaxivity R1 depends more preferentially on the total surface area of the nanoparticles than on the particle size. Recently, enhanced T1 contrast was found in MnO nanoparticles when the particle size was decreased [98], and also higher surface-to-volume structures were obtained in which more active magnetic ions were exposed to water protons, exhibiting much higher R1 values [99].

(iii) Surface properties: the magnetic interactions between water and nanoparticles occur preferentially at the particle surface, so it is perfectly understandable that the use of capping agents that modify or functionalize the surface plays an important role in the magnetic properties and, therefore, in the MRI contrast enhancement. They affect the relaxation of the water molecules in several

ways, for example, favoring the diffusion of the protons to the magnetic core or also establishing hydrogen bindings. This is especially important in the nanoparticles used for in vivo experiments, since they must be biocompatible and show as low toxicity as possible. As mentioned above, there are a lot of coating materials and strategies commonly used to functionalize magnetic nanoparticles for in vivo applications. Regarding the MR imaging, hydrophobicity and shell thickness around the nanoparticle are two important factors that determine the efficiency of the enhanced MRI contrast [100, 101].

According to Koening-Keller model, the longitudinal (spin-lattice, energy exchange between water and paramagnetic ions) or transverse (spin-spin, dipolar magnetic interaction between the water proton spins and the magnetic moment of the nanoparticle) relaxivity R_i can be expressed as following [102]:

$$R_i = \frac{1}{T_i} = \frac{a}{d_{MNP}D}\gamma^2\mu^2 C_{MNP} J(\omega, \tau_D) \quad (i = 1, 2) \tag{15.2}$$

Where a is a constant, d_{MNP} is the diameter of the magnetic nanoparticle, D is the diffusion coefficient of water, μ is the magnetic moment of the nanoparticles, γ is the gyromagnetic ration of the water proton, C_{MNP} is the concentration of the nanoparticles, and $J(\omega,\tau_D)$ is the spectral density function.

Magnetic nanoparticles possess unique structural and magnetic properties that confer them with ability to interact with cells and biomolecules, making them very interesting platforms to be used in many biomedical applications. In particular, they have been carefully studied over the past few years as contrast agents for MRI applications, such as cancer imaging, cell migration, gene expression, angiogenesis, apoptosis, cardiovascular disease imaging, or molecular imaging [103]. High-resolution molecular and cellular imaging is one of the most promising applications of magnetic nanoparticles due to their powerful ability to diagnose diseases in early stages of progress, by combining molecular biology and in vivo imaging [104]. Advances in particle surface functionalization have provided nanoparticles with ligands having functional moieties able to recognize molecular and cellular targets. In this way, MNP-based molecular imaging offers a noninvasive visual representation beyond the vascular and tissue morphology imaging, providing a high-resolution monitoring of the expression and activity of specific molecules and biological processes at the cellular and molecular levels, such as in vivo cell tracking [105, 106] angiogenesis, metastasis, apoptosis detection [107, 108], and imaging of enzyme activities [109], that determine tumor behavior and response to therapy. Furthermore, these MNPs with targeted moieties can be also loaded with drugs, in such a way that they can recognize diseases (i.e., tumors) at molecular or cellular levels and play simultaneous diagnosis and treatment roles more efficiently that can be visually followed. For all of these characteristics, these multifunctional nanoplatforms become really helpful on cancer detection, allowing an individualized therapeutic treatment of the patient and drug development. It is important to remark the outstanding spatial resolution of MRI that, for example, in oncology

diagnosis applications, allows to detect millimeter-sized metastases, which is beyond the detection limit of other imaging techniques [110].

Hyperthermia

Hyperthermia refers to an abnormally high temperature found in a body, which can be of natural origin, as in any fever process, or be artificially produced to obtain therapeutical benefits. Induced hyperthermia goes back far in time to the Greek's and Roman's physicians who believed that they could cure any disease by controlling the body temperature [111].

This inspiration took concrete form in modern medicine through multiple techniques using extended sources, as infrared or microwave techniques, to help killing cancer cells by rising the body temperature above 42–45 °C. However, these approaches resulted to be nonspecific and provoked harmful secondary effects in the healthy tissues. This encouraged the search of new mechanisms capable of increasing the T of damaged areas while keeping healthy the rest of tissues. And one solution to this was found with magnetic hyperthermia and the use of magnetic nanoparticles. Magnetic hyperthermia allows to remotely induce local heat by means of the magnetic energy losses of MNP under an oscillating magnetic field. In other words, magnetic nanoparticles are able to transform electromagnetic energy into heat (Fig. 15.7). The frequencies of this oscillating magnetic field must be in the RF field, ranging from a few KHz and 1 MHz. Actually, it is a compromise between healthy radiation and a proper penetration depth into the human body, allowing the access to internal tissues and organs. It also avoids the deleterious physiological responses to high-frequency magnetic fields which include stimulation of the peripheral and skeletal muscles, cardiac stimulation, and arrhythmia [112]. It can be used with confidence for medical therapy if magnetic actuators fulfill the safety regulation requirement to be below a limiting value of $H \cdot f < 4.58 \cdot 10^8$ $A \cdot m^{-1} \cdot s^{-1}$ [113].

Basically, magnetic hyperthermia allows for [114, 115]:

(i) A localized heating of the nanoparticle-containing tissues
(ii) The selective killing of targeted cancer cells, which are thermally more sensitive than the healthy ones
(iii) A considerable reduction of many of the classical secondary effects: killing of healthy cells, long times of exposure to heating sources, or large doses of chemicals into patient's body

Although we will explain deeper the main mechanisms involved in the magnetic losses of magnetic nanoparticles that enable magnetic hyperthermia, we introduce here that they are basically three depending on the electric and magnetic properties of the materials:

(i) Eddy currents: induced in the material if this has appreciable conductivity.
(ii) Hysteresis losses: this is the main mechanism in nonconductive FM particles, involving magnetic domain creation and motion and extinction processes. In a simple approach, they can be easily quantified by the area under the MvsH hysteresis loop.

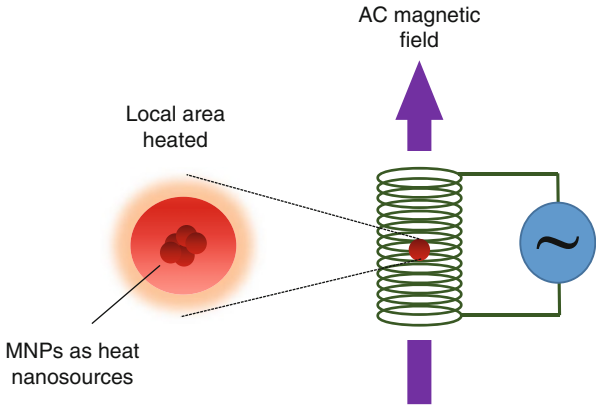

Fig. 15.7 Illustration of MNP-based hyperthermia

(iii) Brown and Néel relaxation times: these are the main mechanisms involved in dispersions consisting of superparamagnetic nanoparticles (particle sizes below the single-to-multidomain transition).

The use of superparamagnetic iron oxide nanoparticles is preferred in biomedical applications for several reasons: they are thought to be biocompatible and nontoxic, they show size-tunable magnetic properties with relatively high saturation magnetizations and noncoercive forces or remanence, preventing magnetic particle interactions and avoiding particle aggregation after removing the applied magnetic field.

The efficiency of MH applications depends on the instrumental parameters (externally applied magnetic field intensity and frequency) and the physicochemical properties of the colloidally stable nanosized systems (particle shape and size, distribution, concentration, embedding medium properties, or chemical, structural, and magnetic properties) [115–117] that have to be optimized for each specific application.

It is important to mention that magnetic hyperthermia as therapy has been successfully installed in some clinics and hospitals. This is the case of a setup developed in Germany [118], which comprises a clinical magnetic actuator together with a therapeutic ferrofluid of optimized iron oxide nanoparticles with an aminosilane coating that provides a fully operative clinical therapy for brain cancer in humans. It constitutes the first European approval for a medical product using magnetic nanoparticles for clinical purposes [4, 118].

Magnetic Hyperthermia Basis

The understanding of the relevant parameters which govern the magnetic hyperthermia performances of MNPs is crucial in order to maximize the heat release. Transformation of magnetic energy into heat can be analyzed in terms of specific absorption rate (SAR), (W/g^{-1}), or the specific loss power, SLP (W/m^{-3}), which are simply related by $\rho = m/V^{-1}$ ($g\ m^{-3}$) [112]. Experimentally this quantity is simply determined applying

thermodynamics by measuring the temperature increase of the system, which is related to the energy transferred to it by

$$Q = m \cdot C \cdot \Delta T = (m \cdot C + m_1 \cdot C_1)\Delta T \tag{15.3}$$

where C and C_1 are respectively the specific heat capacity per unit mass of the medium and magnetic material: $V_1 = m_1/\rho$. This quantity is related to magnetic power density, P, applied to the system by $Q/t = P \cdot V_1$, and leads to the experimental expression for SAR, which is easily determined by measuring the temperature increase of the system by

$$SAR = \frac{P \cdot V_1}{m_1} = \frac{P}{\rho} = \frac{(m \cdot C + m_1 \cdot C_1)}{m_1} \cdot \frac{\Delta T}{\Delta t} \tag{15.4}$$

Although the experimental determination of SAR is very simple, the challenge is to formulate it in terms of the applied magnetic excitation and the colloidal parameters of the ferrofluid in order to be able to optimize the performance for each precise application. The first approaches that attempt the quantification of SAR relay on the fact that small nonconducting MNPs respond linearly to the low-amplitude magnetic field excitations which are used in biomedical applications [119]. The well-known approach of Rosensweig [120] relays on this assumption and bases magnetic hyperthermia on relaxation processes for superparamagnetic (SPM) diluted ferrofluids and hysteretic dissipation in large FM-based ferrofluids. Since then, the limits of validity of the assumption of linear response have been questioned and on the last years new contributions to the field have been proposed under a more comprehensive view which intend to give a complete view of SAR produced by MNPs of any size, from SPM to FM [121, 122].

The Rosensweig's approach assumes that transformation of radio-frequency (RF) magnetic energy into heat by MNPs is due to different processes depending on the size: hysteresis losses due to magnetic domain and domain wall motion for multidomain nanoparticles, respectively [120]. And Néel and Brown relaxation mechanisms for single-domain SPM (superparamagnetic).

In multidomain particles (ferro- or ferrimagnetic), each magnetic domains has a definite direction of magnetization, which under the application of a magnetic field, changes promoting the growth of those domains with a magnetization direction along the applied magnetic field axis. This process, sketched in Fig. 15.8, is irreversible and energy losses take place as magnetization follows, in an hysteretic fashion, the cycles of the AC applied magnetic field. In this way, SAR can be easily calculated from experimental data as

$$P(H,f) = A_{hys} f \tag{15.5}$$

For particle sizes below the superparamagnetic (SPM) limit, no magnetization hysteresis appears and, therefore, no heating due to hysteresis losses occur. In this scenario, an externally applied magnetic field may produce two different effects:

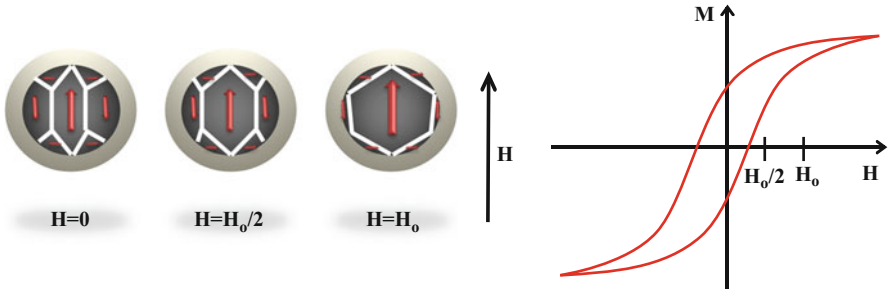

Fig. 15.8 (*left*) Magnetization grows in the direction of the applied magnetic field on multidomain MNPs (*right*) FM hysteresis loop responsible for the irreversible energy losses by reversal magnetization cycles

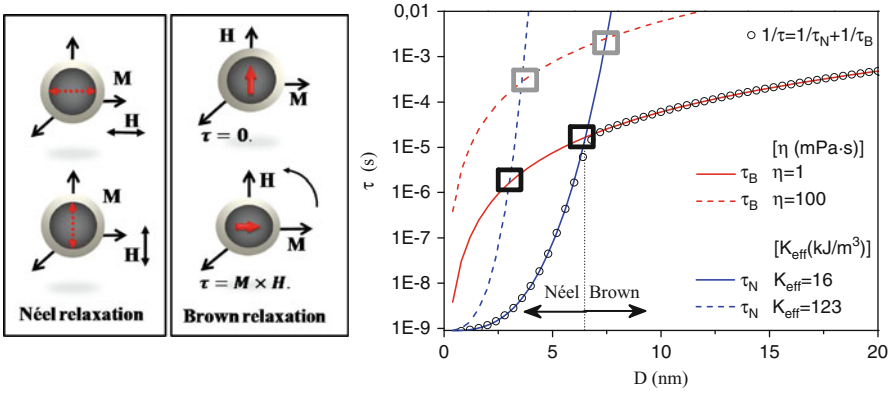

Fig. 15.9 (*left*) Néel and Brown relaxation mechanisms and (*right*) and characteristic times τ, τ_N, and τ_B as a function of NPs size calculated for magnetite parameters

(i) If it can overcome the energy barrier $E_b = KV$ of the particle, it will reorient internally M inside the crystal lattice. (ii) If, otherwise, the energy barrier is much higher, magnetization will remain in the direction minimum energy and the magnetic field will physically rotate the whole particle within the solvent following the torque, $\boldsymbol{\tau} = \boldsymbol{M} \times \boldsymbol{H}$ provoking the subsequent heat losses by reversal magnetization or friction, respectively.

These mechanisms, sketched in Fig. 15.9, are respectively known as Néel and Brown relaxations, with a characteristic times, τ_N and τ_B, defined by

$$\tau_N = \tau_0 \frac{\sqrt{\pi}}{2} \frac{\exp\left(\frac{K_{eff}V}{k_B T}\right)}{\left(\frac{K_{eff}V}{k_B T}\right)^{1/2}} \tag{15.6}$$

$$\tau_B = \frac{3\eta V_H}{k_B T} \tag{15.7}$$

where η is the viscosity of the solvent in which the particles are dispersed, k_B the Boltzmann constant, T the absolute temperature ($\boldsymbol{K}$), $\boldsymbol{V_H}$ the hydrodynamic volume of the particle (including the nonmagnetic shell if exists), and V the magnetic volume of the core and K_{eff} effective anisotropy constant. Both mechanisms depend on particle size whereas only the Brownian contribution depends on the viscosity, η, of the embedding medium. Rosensweig assumed that both may contribute as processes occurring in parallel and their combination is accounted into an effective relaxation time $\frac{1}{\tau} = \frac{1}{\tau_B} + \frac{1}{\tau_N}$ to produce losses as follows:

$$P = \Delta U f = \frac{H_0^2 \mu_0^2 V M_s^2}{3 k_B T \tau} \frac{(2\pi f \tau)^2}{1 + (2\pi f \tau)} \tag{15.8}$$

In Figure 15.9 the Brown, Néel and effective relaxation times are illustrated by computing equations (15.6) and (15.7) for different experimental conditions: maghemite NPs with $K_{eff} = 16$ kJ/K and cobalt ferrite with $K_{eff} = 123$ kJ/K solved in water with $\eta_{\text{water}} = 1$ mPa·s and a viscous mixture $\eta_{\text{water}} = 100$ mPa·s at $T = 293$ K.

The crossover between both regimes ($\tau_N = \tau_B$), marked with squares in the figure, depends on the effective anisotropy and the viscosity of the solvent and determines which mechanism will prevail in each case. For example, strong magnets (higher K_{eff}) will show more contribution from Brown relaxation since anisotropy energy barrier is large and Néel relaxation will happen very much slowly (large τ_N). In addition for highly viscous fluids, Brown relaxation will be highly hindered, (large τ_B), and Néel relaxation will lead the heat release.

Parameters Influencing the Performance of MH in Biological Environments

In biological environments such as blood, tumor cells, or in the extracellular matrix which is a highly complex medium composed by many types of macromolecules, viscosity is high and largely variable compared to the usual water-based ferrofluids, η(water) = [1] mPa·s, employed to validate the theoretical models of magnetic hyperthermia. For example, blood is three times more viscous than water, η(blood) = [3,4] mPa·s [123], and in different cell locations viscosity can vary from low η(cytoplasm) = [1,3] mPa·s, in the cytoplasm, up to large viscosity in extracell matrix η(matrix) = 200 mPa·s, i.e., SK-OV-3 ovarian cancer cells present viscosities among η(SK-OV-3) = [120,260] mPa·s [124]. Therefore, an adequate experimental design of in vitro and in vivo MH applications requires a systematic study of the physicochemical parameters involved in the SAR performance, with values simulating the conditions of biological environments:

(i) Variable range of viscosities: $\eta = [1, 400]$ mPa·s.
(ii) MNPs are locally concentrated on the target location $\Phi = [0.1, 100]$ g/L^{-1}.
(iii) Small sizes to avoid the immune system $D = [1, 30]$ nm.

Despite of its limits of applicability, Rosensweig's model is mathematically more affordable than others and can be used to obtain general predictions about the influence of the physicochemical conditions on the heat release. There can be found in literature computations of SAR given by Eq. 15.8 Rosensweig [120, 125] varying widely the range of the parameters [126]. However, only brief results about the general behavior of SAR with respect to viscosity, particle size, concentration, and coating are presented here, since an exhaustive analysis of this subject is beyond the intention of this handbook. Therefore, within the Rosensweig model [120], there is generally predicted that (i) an optimum viscosity exists for which losses can be maximized, which remains nearly independent of the applied field magnitude but moves to lower values for large frequencies and large particles [125] and (ii) an optimum particle size (R and RH) exists which stands nearly independent of the applied field, although polydispersity widens the shape of the peak and its location and magnitude depend respectively on viscosity and frequency [125].

To find the location of the optimum viscosity or size, one can analyze the condition of maximum of losses:

$$2\pi f = {}^{1}\!/\!_{\tau_N}\left(K_{eff},R\right)+{}^{1}\!/\!_{\tau_B}\left(\eta,R\right) \tag{15.9}$$

This readily shows the intricate behavior among all parameters, which are in the origin of much part of the experimental controversies found in literature. In fact, depending on particular combinations of the experimental parameters, the profile of SAR can present a maximum, be flat, or even decay. In Figure 15.10, computations of normalized SAR versus viscosity η, for magnetite MNPs, illustrate how frequency and size can shift the maximum towards lower values of η when frequency is increased in Fig. 15.10 (left), or size is increased in Fig. 15.10 (right). However, for a different combination of experimental conditions, location of maximums or shape and magnitude of SAR can largely vary.

Reported SAR data [126], for dextran-coated magnetite based ferrofluids, show a significant dependence of losses with viscosity, from the lowest loss value $P = 57$ W/g^{-1} on $\eta = 1$ mPa.s to the maximum $P_{\max} = 76$ W/g^{-1} on $\eta = 1.96$ mPa·s. In another work [17], reported experimental data of polyacrylic acid-coated magnetite MNPs in water show a milder dependence on viscosity. The location of the maximum in this case was reported on $\eta = 17$ mPa.s with a loss value of SAR = 37.2 W/g^{-1}. The decrease in SAR is due to the mechanical hindrance that increases with large viscosities producing a decay in the contribution of Brown relaxation. And, also marginal dependences on viscosity have been observed by Wang et al. [127], as reported in Table 15.1, for magnetite NPs ferrofluids in different solvents.

A further step was given by Fortin et al. [116, 128] in an interesting study made with γ-Fe_2O_3 maghemite and $CoFe_2O_4$ cobalt ferrite which were internalized into cultured tumor cells and exposed under MH. Both compositions entered with the same efficiency and were uptake by endosomes of 0.5 μm and confined there on high concentrations. In order to unravel the mechanism of the intracellular heating, sets of NPS with sizes in between $D = [7, 15]$ nm were dispersed in different

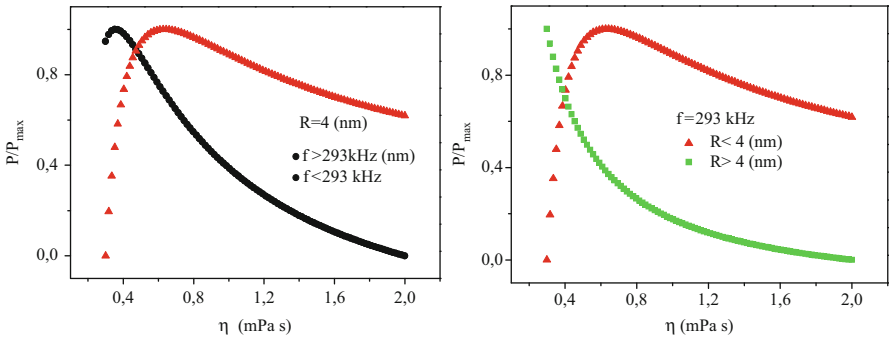

Fig. 15.10 Normalized losses obtained with simulations of Rosensweig's equation for different experimental conditions

Table 15.1 SAR data reported in Ref. [127] for magnetite ferrofluids showing the influence of solvents' viscosity

	η (mPa s) solvent				
Core D (MNP)	SAR (W/g^{-1})				
Magnetite 10 nm	0.545 Octane	0.586 Toluene	0.601 Benzene	0.696 Styrene	38.8 Oleic acid
	123	127	135	124	126

mixtures of water and glycerol covering large range of viscosities $\eta = [1, 1{,}000]$ mPa s and simulating different cell environments. In Fig. 15.11, it is only shown the behavior of SAR for small NPS of maghemite, $D = 7.1$ nm, and cobalt ferrite, $D = 9.7$ nm, although results for other sizes can be seen in Ref. [130]. Generally, SAR maghemite NPs shows to be independent of η into the experimental conditions while cobalt ferrite decays steeply for small sizes and afterwards presents a slight increase up to a plateau for large sizes. These results in combination with the fact that anisotropy constants for both materials are largely different, $K_{eff}(\gamma\text{-}Fe_2O_3) = 16$ kJ/m^{-3} and $K_{eff}(Co\ Fe_2O_4) = 123$ kJ/m^{-3}, allowed them to conclude that maghemite nanoparticle generates heat mostly by Néel relaxation and cobalt ferrite by Brown relaxation. And therefore, for intracellular environment, where viscosity is so large that Brown relaxation is mostly hindered, maghemite will be the most suitable material, since it mainly contributes with Néel relaxation (unaffected by viscosity). In fact, in their study maghemite NPS of 14 nm attain large losses, around 1,000 W/g^{-1}.

Another important parameter influencing the heating performance is size, through the intricate relationship reported above, Eq. 15.9. Experimental results show that SAR confirms Rosensweig's prediction, although, as it happens with viscosity, the location of the optimum size depends strongly on the rest of the experimental parameters. In Fig. 15.12, a compilation of different experimental data of the heat losses, SAR, reported in literature [125, 129, 130], is plotted for magnetite NPs with different sizes. It can be observed the

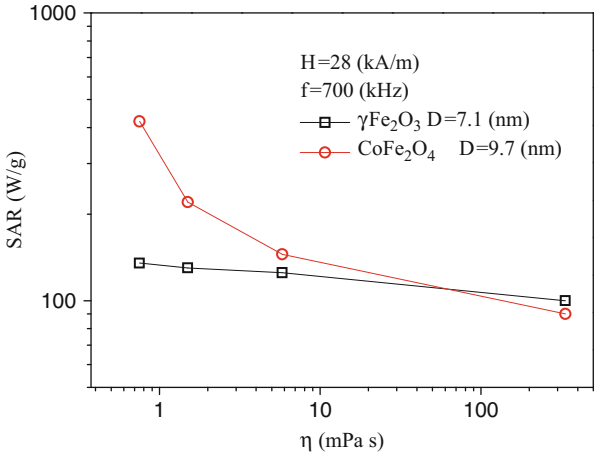

Fig. 15.11 SAR for small NPS of maghemite, $D = 7.1$ nm, and cobalt ferrite, $D = 9.7$ nm, dispersed in mixtures of water and glycerol with $\eta = [1, 1{,}000]$ mPa s, plotted from experimental data reported on Fortin et al. [128]

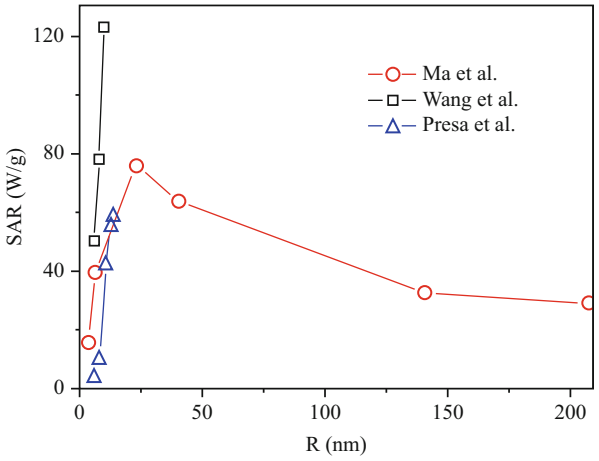

Fig. 15.12 Experimental dependence of SAR with size for magnetite NPs from data reported in literature

dependence on size, which for the experimental conditions in Ma et al. [129] the maximum of SAR is attained around 20 nm. For larger sizes the losses decrease mainly due to an increase volume (and so the anisotropy energy barrier), which makes the Néel relaxation process less effective.

Another example is given by Motoyama et al. [131] in Fig. 15.13, which shows the influence of particle size and frequency on the behavior of SAR (W/g^{-1}). SAR experimental data of a set of magnetite NPs were plotted versus the specific surface areas (SSA), which are directly related to particle size. The effect of frequency on the location and magnitude of the maximum of SAR for a fixed applied magnetic power (6 kW) are evident.

Since surface spins in typical 10 nm nanoparticles represent the third part of the total [132], the chemical environment of surface contributes importantly to the

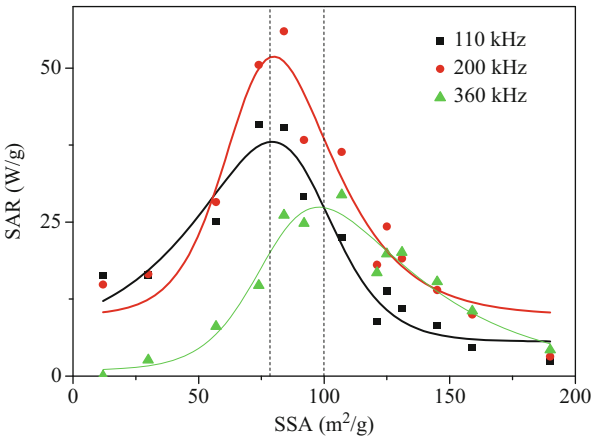

Fig. 15.13 SAR (W/g^{-1}) data reported by Ref. [131] about a set of magnetite NPS with different specific surface areas (*SSA*), directly related to size, and under different frequencies and a total magnetic field power 6 kW

particle properties and the coating shell can affect the magnetic hyperthermia performance through different ways:

(i) By the magnetic interaction of spins between the NP surface and the coating agent, which can alter the inner spins configuration by exchange bias from the surface to the core [133].

(ii) Due to the shell thickness and the physical properties of the coating, which can hinder the heat transference from the inside of the particle to the outside or induce hydrodynamic hindrances.

Some of the influences of the coating are not computed into the Rosensweig's model, i.e., the thermal conductivity of the shell or the magnetic deviation produced to the core properties. Therefore, detailed experimental testing of the coating materials is needed before attempting to design hyperthermia applications. It has been reported by Guardia et al. [133] that very small magnetite NPs $D = [6,20]$ nm, coated with oleic acid, show a saturation magnetization, M_{sat}, around 80 emu/g^{-1}, very close to the bulk value 82 emu/g^{-1}, larger than expected for small NPs. They attribute unexpectedly high value to the covalent bonding of oleic acid molecules to the surface of magnetite that attains to reduce the spin disorder at the surface. Interestingly, Wang et al. [127], in a different work, report SAR values for magnetite NPs, which we include in Table 15.2, coated with different materials, revealing that those coated with oleic acid present the best MH performance. This fact is in clear correspondence with the magnetic order enhancement that oleic acid provides to the NPs surface as measured by Guardia et al. [133].

On the other hand, surface spins may get pinned in a disordered state by the coating and by exchange bias effect, they also transfer some degree of frustration or disorder to the core spins, lowering the total magnetization of the nanoparticle. If this happens, the expected magnetic heating power will be worst. The effect of coating is crucial for drug delivery applications triggered by magnetic hyperthermia, since the effectiveness of the delivery depends of the magneto-thermal ability of the ensemble. Therefore, thermally active coating has to preserve the

Table 15.2 Effect of coating materials on SAR for magnetite NPs reported in Ref. [127]

	Surfactants			
Core D (MNP)	SAR (W/g^{-1})			
Magnetite 10 nm	None	Amilosane	Oleic acid	Oleic acid + SDBS
	21	77	126	120

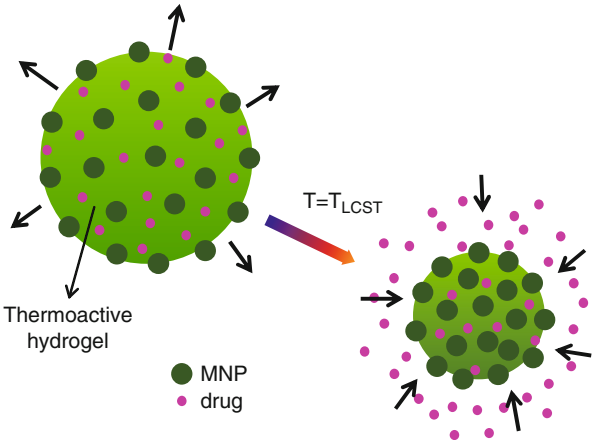

Fig. 15.14 Example of a drug delivery mechanism induced by magnetic hyperthermia

magnetic properties of the MNP core to be properly triggered by the magnetic action of the core. Poly-*N*-isopropylacrylamide (PNIPAM) is a biocompatible and thermo-reversible polymer able to generate hydrogels that undergo a coil to globule collapse for temperatures above 32 °C (which called the lower critical solution temperature LCST) [134]. The coil collapse can be exploited to expel substances (Fig. 15.14). In fact, conveniently loaded with therapeutic agents and magnetic cores, PNIPAM is the preferred candidate in drug delivery applications. Regmi et al. [135] have loaded PNIPAM/magnetite composites with mitoxantrone, an anticancer drug, and have succeeded to produce a controlled release of the drug by applying magnetic hyperthermia. By applying a magnetic field of 130 (Oe) and 380 kHz, on samples with different compositions in PNIPAM/magnetite loaded with mitoxantrone, they attained to produce a mild hyperthermia from 298 to 323 K in only 4 min and a controlled release of the drug up to the 4 % of the total [135].

Another source of controversy is the influence of magnetic material concentration on the MH performance. Obviously, below a certain concentration there is no appreciable temperature increase upon the application of a magnetic field over a ferrofluid. For biological environments this is a crucial factor for having success. Fortin et al. [128] incubated cancer cells with maghemite, with a proportion of 22.6 pg per cell, into pellets of 300 μL containing 20 million cells. For different percentages of magnetized cells $\Phi = [0, 20, 80, 100]$ %, by application of MH the temperature raised from $T_{in} = 37$ °C to $T_f = [37.5, 38.5, 43, 44.5]$ °C.

However the controversy rises up for the concentration effects on the efficiency of the heating, SAR. Examples can be found in literature where for magnetite ferrofluids marginal dependences of SAR versus concentration are found (Uritzberea et al.) [136]; sharp losses are observed in Linh et al. [137], or even maximums of SAR depending on experimental conditions have been reported for iron NPs [138]. There is no common theoretical frame explaining this controversy, since it is a complex task involving the interplay of dipolar interactions on non-touching particles, exchange interactions in contacting NPs, anisotropy, and thermal energies.

Conclusions and Future Remarks

The development of the nanotechnology has allowed a drastic miniaturization of the materials and opened new frontiers for applications. The multidisciplinary approach carried out over the last decades to address fundamental and applied issues at the nanoscale have boosted the research on single nanoplatforms that are able to integrate several functionalities. This is the case of the so-called 'theranostic' nanoparticles in the biomedical field, which are able to carry out simultaneously diagnosis and therapeutic functions in diseased areas of the human body.

In this chapter we have focused on iron oxide-based nanoparticles, since they constitute the most widely accepted magnetic nanoparticles for in vivo biomedical applications due to their unique size-dependent magnetic properties, biocompatibility, and ability to be easily surface modified with both organic and inorganic coating agents. Therefore, a delicate design of structure, composition, and surface chemistry is essential to achieve the desired properties in MNP systems, such as chemical stability, specific target recognition (molecules, cells, diseased tissues), and/or multimodality, that will enable their efficient performance in final applications, such as hyperthermia and high MR imaging-contrast, both reviewed in this chapter as two of the main researched applications of magnetic nanoparticles in biomedicine. In general, the most efficient nanostructures for biomedical applications using magnetic nanoparticles consist of (i) a magnetic core responsible of the required magnetic behavior, (ii) water-soluble surface that provides them stability and compatibility in physiological fluids, and (iii) surface functionalized with bioactive ligands for specific targeting purposes. The design of these magnetic nanosystems is especially interesting in hyperthermia and MRI applications, as more efficient nanoheaters and contrast agents for MRI, respectively. The combination of adequate magnetic properties with a proper particle surface functionalization for specific target recognition not only will allow the detection of diseases in early stages of advance but also to monitor molecules and biological processes characteristic of specific evolution stages of the disease, as well as to provide a more localized therapeutic treatment (i.e., magnetically induced drug delivery) which effectiveness can be also followed in situ.

With the development of nanotechnology, novel physicochemical properties and applications have been emerging. Although it is difficult to speculate about what kind of new discoveries at the nanoscale the future will bring us, the logical advance in the particular case of magnetic nanoparticles for biomedical applications seem to be the development of multifunctional and more complex nanosystems able to more efficiently overcome several limitations that are being found today by using more simple structures. The knowledge achieved about the synthesis and nanoparticle surface functionalization has boosted the development of detection systems based on the ability of magnetic nanoparticles to recognize and attach specific targets. In the particular case of magnetic hyperthermia and MRI, the design of nanoparticle-based structures that combine a magnetic core and suitable functional moieties remains promising for a simultaneous high sensitivity detection and high space resolution for localized treatment and/or imaging. Actually, the combination of several materials with different magnetic properties in one single structure continues to be a challenge in order to obtain more efficient contrast agents that simultaneously enhance both T1 and T2 MR contrast. The accumulation of these systems in desired tissues and organs will allow us to focus more precisely in the damaged cells and leave healthy the surrounding ones. In the case of hyperthermia, a specific attachment of these heat nano-generators to the tissue of interest is essential. In this sense, the specificity shown by many toxins could be a very suitable driven force for targeting of these multifunctional nanosystems. It is also important to mention the use of hyperthermia technology as a promising tool for drug delivery systems, in which the drug release is achieved by a temperature increase magnetically induced.

However, a new world starts to be explored below nanometer scale: *atomic clusters*. In the last years, the synthesis of sub-nanometric metal clusters (Au, Ag, Cu) has been greatly investigated due to their amazing chemical, optical, and catalytic properties [139]. At this particle-size scale, their physicochemical behavior is dominated by quantum effects, which are responsible of a drastic change of their chemical, optical, and electrical properties (magnetism, photoluminescence, or catalytic activity). All these unique properties make sub-nanometric species very promising for biomedical applications. For example, their very small size could overcome problems related to overpass physiological barriers, whereas the possibility of having magnetic clusters could provide new original solutions for molecular MRI.

Acknowledgments The authors would like to thank Prof. Carlos Vázquez-Vázquez for the critical reading of this manuscript. Undoubtedly, his comments have contributed to a significant quality improvement of this chapter.

References

1. Ko SH, Park I, Pan H, Grigoropoulos CP, Pisano AP, Luscombe CK, Fréchet JMJ (2007) Direct nanoimprinting of metal nanoparticles for nanoscale electronics fabrication. Nano Lett 7(7):1869

2. Gibson RF (2010) A review of recent research on mechanics of multifunctional composite materials and structures. Compos Struct 92:2793
3. Bañobre-López M, Piñeiro-Redondo Y, De Santis R, Gloria A, Ambrosio L, Tampieri A, Dediu V, Rivas J (2011) Poly(caprolactone) based magnetic scaffolds for bone tissue engineering. J Appl Phys 109:07B313
4. Rivas J, Bañobre-López M, Piñeiro-Redondo Y, Rivas B, López-Quintela MA (2012) Magnetic nanoparticles for application in cancer therapy. J Magn Magn Mater 324:3499
5. Laurent S, Forge D, Port M, Roch A, Robic C, Vander Elst L, Muller RN (2008) Magnetic iron oxide nanoparticles: synthesis, stabilization, vectorization, physicochemical characterizations, and biological applications. Chem Rev 108(6):2064
6. Hadjipanayis CG, Bonder MJ, Balakrishnan S, Wang X, Mao H, Hadjipanayis GC (2008) Metallic iron nanoparticles for MRI contrast enhancement and local hyperthermia. Small 4(11):1925
7. Langer R (1990) New methods of drug delivery. Science 249(4976):1527
8. Bulte JWM, Modo MMJ (eds) (2008) Nanoparticles in biomedical imaging – emerging 1009 technologies and applications. Springer, New York
9. Lu AH, Salabas EL, Schüth F (2007) Magnetic nanoparticles: synthesis, protection, functionalization, and application. Angew Chem Int Ed 46(8):1222
10. Salgueiriño-Maceira V, Correa-Duarte MA (2007) Increasing the complexity of magnetic core/shell structured nanocomposites for biological applications. Adv Mater 19(23):4131
11. LaMer VK, Dinegar RH (1950) Theory, production and mechanism of formation of monodispersed hydrosols. J Am Chem Soc 72(11):4847
12. den Ouden CJJ, Thompson RW (1991) Analysis of the formation of monodisperse populations by homogeneous nucleation. J Colloid Interface Sci 143(1):77
13. Sugimoto T, Matijevic E (1980) Formation of uniform spherical magnetite particles by crystallization from ferrous hydroxide gels. J Colloid Interface Sci 74(1):227
14. Ocaña M, Rodriguez-Clemente R, Serna CJ (1995) Uniform colloidal particles in solution: formation mechanisms. Adv Mater 7(2):212
15. Lee J-H, Huh Y-M, Y-w J, J-w S, J-t J, Song H-T, Kim S, Cho E-J, Yoon H-G, Suh J-S, Cheon J (2007) Artificially engineered magnetic nanoparticles for ultra-sensitive molecular imaging. Nat Med 13:95
16. Cushing BL, Kolesnichenko VL, O'Connor CJ (2004) Recent advances in the liquid-phase syntheses of inorganic nanoparticles. Chem Rev 104(9):3893
17. Piñeiro-Redondo Y, Bañobre-López M, Pardiñas-Blanco I, Goya G, López-Quintela MA, Rivas J (2011) The influence of colloidal parameters on the specific power absorption of PAA-coated magnetite nanoparticles. Nano Res Lett 6:383
18. Zhang Y, Kohler N, Zhang M (2002) Surface modification of superparamagnetic magnetite nanoparticles and their intracellular uptake. Biomaterials 23(7):1553
19. Petri-Fink A, Chastellain M, Juillerat-Jeanneret L, Ferrari A, Hofmann H (2005) Development of functionalized superparamagnetic iron oxide nanoparticles for interaction with human cancer cells. Biomaterials 26(15):2685
20. D'Souza AJM, Schowen RL, Topp EM (2004) Polyvinylpyrrolidone-drug conjugate: synthesis and release mechanism. J Control Release 94(1):91
21. Berry CC, Wells S, Charles S, Aitchison G, Curtis ASG (2004) Cell response to dextran-derivatised iron oxide nanoparticles post internalisation. Biomaterials 25(23):5405
22. Bergemann C, Müller-Schulte D, Oster J, Brassard L, Lübbe AS (1999) Magnetic ion-exchange nano- and microparticles for medical, biochemical and molecular biological applications. J Magn Magn Mater 194(1–3):45
23. Rodríguez C, Bañobre-López M, Kolen'ko YV, Rodríguez B, Freitas P, Rivas J (2012) Magnetization drop at high temperature in oleic acid-coated magnetite nanoparticles. IEEE Trans Magn 48(11):3307

24. Hyeon T, Lee SS, Park J, Chung Y, Na HB (2001) Synthesis of highly crystalline and monodisperse maghemite nanocrystallites without a size-selection process. J Am Chem Soc 123(51):12798
25. Sun S, Zeng H (2002) Size-controlled synthesis of magnetite nanoparticles. J Am Chem Soc 124(28):8204
26. Sun S, Zeng H, Robinson DB, Raoux S, Rice PM, Wang SX, Li G (2004) Monodisperse MFe_2O_4 (M = Fe, Co, Mn) nanoparticles. J Am Chem Soc 126(1):273
27. Park J, An K, Hwang Y, Park J-G, Noh H-J, Kim J-Y, Park J-H, Hwang N-M, Hyeon T (2004) Ultra-large-scale syntheses of monodisperse nanocrystals. Nat Mater 3(12):891
28. Li Z, Sun Q, Gao M (2005) Preparation of water-soluble magnetite nanocrystals from hydrated ferric salts in 2-pyrrolidone: mechanism leading to Fe_3O_4. Angew Chem Int Ed 44(1):123
29. Hu F, Wei L, Zhou Z, Ran YL, Li Z, Gao M (2006) Preparation of biocompatible magnetite nanocrystals for in vivo magnetic resonance detection of cancer. Adv Mater 18(19):2553
30. López-Quintela MA, Rivas J (1993) Chemical reactions in microemulsions: a powerful method to obtain ultrafine particles. J Colloid Interface Sci 158(2):446
31. López-Quintela MA, Rivas J (1996) Nanoscale magnetic particles: synthesis, structure and dynamics. Curr Opinion Colloid Interface Sci 1(6):806
32. López-Quintela MA, Rivas J, Blanco MC, Tojo C (2003) Synthesis of nanoparticles in microemulsions. In: Liz Marzán LM, Kamat PV (eds) Nanoscale materials, vol 6. Kluwer Academic Plenum, Dordrecht, Netherlands, p 135
33. López-Quintela MA (2003) Synthesis of nanomaterials in microemulsions: formation mechanisms and growth control. Curr Opin Colloid Interface Sci 8(2):137
34. Boutonnet M, Kizling J, Stenius P (1982) The preparation of monodisperse colloidal metal particles from microemulsions. Colloids Surf A: Physicochem Eng Aspects 5(3):209
35. Woo K, Lee HJ, Ahn J-P, Park YS (2003) Sol–gel mediated synthesis of Fe_2O_3 Nanorods. Adv Mater 15(20):1761
36. Vidal J, Rivas J, López-Quintela MA (2006) Synthesis of monodisperse maghemite nanoparticles by the microemulsion method. Colloids Surf A Physicochem Eng Asp 288 (1–3):44
37. López-Pérez JA, López-Quintela MA, Mira J, Rivas J, Charles SW (1997) Advances in the preparation of magnetic nanoparticles by the microemulsion method. J Phys Chem B 101(41):8045
38. Wang X, Zhuang J, Peng Q, Li Y (2005) A general strategy for nanocrystal synthesis. Nature 437(7055):121
39. Deng H, Li X, Peng Q, Wang X, Chen J, Li Y (2005) Monodisperse magnetic single-crystal ferrite microspheres. Angew Chem Int Ed Engl 44(18):2782
40. Tartaj P, del Puerto-Morales M, Veintemillas-Verdaguer S, González-Carreño SCJ (2003) The preparation of magnetic nanoparticles for applications in biomedicine. J Phys D: Appl Phys 36:R182
41. Denizot B, Tanguy G, Hindre F, Rump E, Lejeune JJ, Jallet P (1999) Phosphorylcholine coating of iron oxide nanoparticles. J Colloid Interface Sci 209(1):66
42. Hansen T, Clermont G, Alves A, Eloy R, Brochhausen C, Boutrand JP, Gatti AM, Kirkpatrick CJ (2006) Biological tolerance of different materials in bulk and nanoparticulate form in a rat model: sarcoma development by nanoparticles. J R Soc Interface 3(11):767
43. Ahamed M (2011) Toxic response of nickel nanoparticles in human lung epithelial A549 cells. Toxicol In Vitro 25(4):930
44. Mehdaoui B, Meffre A, Lacroix L-M, Carrey J, Lachaize S, Gougeon M, Respaud M, Chaudret B (2010) Large specific absorption rates in the magnetic hyperthermia properties of metallic iron nanocubes. J Magn Magn Mater 322(19):L49
45. Deng M, Tu N, Bai F, Wang L (2012) Surface functionalization of hydrophobic nanocrystals with one particle per micelle for bioapplications. Chem Mater 24(13):2592

46. Euliss LE, Grancharov SG, O'Brien S, Deming TJ, Stucky GD, Murray CB, Held GA (2003) Cooperative assembly of magnetic nanoparticles and block copolypeptides in aqueous media. Nano Lett 3(11):1489
47. Liu X, Guan Y, Ma Z, Liu H (2004) Surface modification and characterization of magnetic polymer nanospheres prepared by miniemulsion polymerization. Langmuir 20(23):10278
48. Hong R, Fischer NO, Emrick T, Rotello VM (2005) Surface PEGylation and ligand exchange chemistry of FePt nanoparticles for biological applications. Chem Mater 17 (18):4617
49. Sahoo Y, Pizem H, Fried T, Golodnitsky D, Burstein L, Sukenik CN, Markovich G (2001) Alkyl phosphonate/phosphate coating on magnetite nanoparticles: a comparison with fatty acids. Langmuir 17(25):7907
50. Kim M, Chen Y, Liu Y, Peng X (2005) Super-stable, high-quality Fe_3O_4 dendron–nanocrystals dispersible in both organic and aqueous solutions. Adv Mater 17(11):1429
51. Kobayasi Y, Horie M, Konno M, Rodriguez-Gonzalez B, Liz-Marzan LM (2003) Preparation and properties of silica-coated cobalt nanoparticles. J Phys Chem B 107(30):7420
52. Lu Y, Yin Y, Mayers T, Xia Y (2002) Modifying the surface properties of superparamagnetic iron oxide nanoparticles through a sol−gel approach. Nano Lett 2(3):183
53. Liu Q, Xu Z, Finch JA, Egerton R (1998) A novel two-step silica-coating process for engineering magnetic nanocomposites. Chem Mater 10(12):3936
54. Cheong S, Ferguson P, Hermans IF, Jameson GNL, Prabakar S, Herman DAJ, Tilley RD (2012) Synthesis and stability of highly crystalline and stable iron/iron oxide core/shell nanoparticles for biomedical applications. Chem Plus Chem 77(2):135
55. Shen L, Laibinis PE, Hatton TA (1999) Bilayer surfactant stabilized magnetic fluids: synthesis and interactions at interfaces. Langmuir 15(2):447
56. Wan M, Li J (1998) Synthesis and electrical–magnetic properties of polyaniline composites. J Polym Sci A Polym Chem 36(15):2799
57. Massart R (1981) Preparation of aqueous magnetic liquids in alkaline and acidic media. IEEE Trans Magn MAG-17:1247
58. Deng J, Ding X, Zhang W, Peng Y, Wang J, Long X, Li P, Chan ASC (2002) Magnetic and conducting Fe_3O_4-cross-linked polyaniline nanoparticles with core-shell structure. Polymer 43:2179
59. Vestal CR, Zhang ZJ (2002) Effects of surface coordination chemistry on the magnetic properties of MnFe(2)O(4) spinel ferrite nanoparticles. J Am Chem Soc 124:14312
60. Dresco PA, Zaitsev VS, Gambino RJ, Chu B (1999) Preparation and properties of magnetite and polymer magnetite nanoparticles. Langmuir 15:1945
61. Schladt TD, Schneider K, Schild H, Tremel W (2011) Synthesis and bio-functionalization of magnetic nanoparticles for medical diagnosis and treatment. Dalton Trans 40:6315
62. Xu Z, Hou Y, Sun S (2007) Magnetic core/shell Fe_3O_4/Au and Fe_3O_4/Au/Ag nanoparticles with tunable plasmonic properties. J Am Chem Soc 129:8698
63. Stöber W, Fink A, Bohn EJ (1968) Controlled growth of monodisperse silica spheres in the micron size range. J Colloid Interface Sci 26:62
64. Tago T, Hatsuta T, Miyajima K, Kishida M, Tashiro S, Wakabayashi K (2002) Novel synthesis of silica-coated ferrite nanoparticles prepared using water-in-oil microemulsion. J Am Ceram Soc 85:2188
65. Medintz IL, Stewart MH, Trammell SA, Susumu K, Delehanty JB, Mei BC, Melinger JS, Blanco-Canosa JB, Dawson PE, Mattoussi H (2010) Quantum-dot/dopamine bioconjugates function as redox coupled assemblies for in vitro and intracellular pH sensing. Nat Mater 9:676
66. Dong A, Ye X, Chen J, Kang Y, Gordon T, Kikkawa JM, Murray CB (2011) A generalized ligand-exchange strategy enabling sequential surface functionalization of colloidal nanocrystals. J Am Chem Soc 133:998
67. Erathodiyil N, Ying JY (2011) Functionalization of inorganic nanoparticles for bioimaging applications. Acc Chem Res 44:925

68. Pileni MP (2001) Magnetic fluids: fabrication, magnetic properties, and organization of nanocrystals. Adv Func Mater 11(5):323
69. Sun SH, Zeng H, Robinson DB, Raoux S, Rice PM, Wang SX, Li GX (2004) Monodisperse MFe_2O_4 (M = Fe, Co, Mn) nanoparticles. J Am Chem Soc 126(1):273
70. Lattuada M, Alan Hatton T (2007) Functionalization of monodisperse magnetic nanoparticles. Langmuir 23:2158
71. von Werne T, Patten TE (2001) Atom transfer radical polymerization from nanoparticles: a tool for the preparation of well-defined hybrid nanostructures and for understanding the chemistry of controlled/"living" radical polymerizations from surfaces. J Am Chem Soc 123(31):7497
72. Marutani E, Yamamoto S, Ninjbadgar T, Tsujii Y, Fukuda T, Takano M (2004) Surface-initiated atom transfer radical polymerization of methyl mthacrylate on magnetic nanoparticles. Polymer 45(7):3321
73. Schmidt AM (2005) Magnetic core-shell nanoparticles by surface-initiated ring-opening polymerization of e-caprolactone. Macromol Rapid Commun 26(2):93
74. Wang B, Xu C, Xie J, Yang Z, Sun S (2008) pH controlled release of chromone from chromone-Fe_3O_4 nanoparticles. J Am Chem Soc 130:14436
75. Frey NA, Peng S, Cheng K, Sun S (2009) Magnetic nanoparticles: synthesis, functionalization, and applications in bioimaging and magnetic energy storage. Chem Soc Rev 38:2532
76. Xie J, Chen K, Lee H-Y, Xu C, Hsu AR, Peng S, Chen X, Sun S (2008) Ultrasmall c(RGDyK)-coated Fe_3O_4 nanoparticles and their specific targeting to integrin $\alpha v\beta_3$-rich tumor cells. J Am Chem Soc 130:7542
77. Ma X, Zhao Y, Liang X-J (2011) Theranostic nanoparticles engineered for clinic and pharmaceutics. Acc Chem Res 44(10):1114
78. Lübbe AS, Bergemann C, Riess H, Schriever F, Reichardt P, Possinger K, Matthias M, Dörken B, Herrmann F, Gürtler R, Hohenberger P, Haas N, Sohr R, Sander B, Lemke A-J, Ohlendorf D, Huhnt W, Huhn D (1996) Clinical experiences with magnetic drug targeting: a phase I study with 4´-epidoxorubicin in 14 patients with advanced solid tumors. Cancer Res 56:4686
79. Na HB, Song IC, Hyeon T (2009) Inorganic nanoparticles for MRI contrast agents. Adv Mater 21(21):2133
80. Caravan P, Ellison JJ, McMurry TJ, Lauffer RB (1999) Gadolinium(III) chelates as MRI contrast agents: structure, dynamics, and applications. Chem Rev 99:2293
81. Sun C, Du K, Fang C, Bhattarai N, Veiseh O, Kievit F, Stephen Z, Lee D, Zhang M (2010) PEG-mediated synthesis of highly dispersive multifunctional superparamagnetic nanoparticles: their physicochemical properties and function in vivo. ACS Nano 4(4):2402
82. Pankhurst QA, Connolly J, Jones SK, Dobson J (2003) Applications of magnetic nanoparticles in biomedicine. J Phys D: Appl Phys 36:R167
83. Stephen ZR, Kievit FM, Zhang M (2011) Magnetite nanoparticles for medical MR imaging. Mater Today 14:330
84. Corot C, Robert P, Idee JM, Port M (2006) Recent advances in iron oxide nanocrystal technology for medical imaging. Adv Drug Deliver Rev 58:1471
85. Sun C, Lee JSH, Zhang M (2008) Magnetic nanoparticles in MR imaging and drug delivery. Adv Drug Deliver Rev 60:1252
86. Bae KH, Lee K, Kim C, Park TG (2011) Surface functionalized hollow manganese oxide nanoparticles for cancer targeted siRNA delivery and magnetic resonance imaging. Biomaterials 32(1):176
87. Yang H, Zhuang Y, Sun Y, Dai A, Shi X, Wu D, Li F, Hu H, Yang S (2011) Targeted dual-contrast T1- and T2-weighted magnetic resonance imaging of tumors using multifunctional gadolinium-labeled superparamagnetic iron oxide nanoparticles. Biomaterials 32:4584
88. J-s C, Lee J-H, Shin T-H, Song H-T, Kim EY, Cheon J (2010) Self-confirming "AND" logic nanoparticles for fault-free MRI. J Amer Chem Soc 132:11015

89. Chambon C, Clement O, Leblanche A, Schoumanclaeys E, Frija G (1993) Superparamagnetic iron oxides as positive MR contrast agents: in vitro and in vivo evidence. J Magn Reson Imaging 11(4):509
90. Taboada E, Rodriguez E, Roig A, Oro J, Roch A, Muller RN (2007) Relaxometric and magnetic characterization of ultrasmall iron oxide nanoparticles with high magnetization. Evaluation as potential T1 magnetic resonance imaging contrast agents for molecular imaging. Langmuir 23(8):4583
91. Gref R, Minamitake Y, Peracchia MT, Trubetskoy V, Torchilin V, Langer R (1994) Biodegradable long-circulating polymeric nanospheres. Science 263:1600
92. Seo WS, Lee JH, Sun X, Suzuki Y, Mann D, Liu Z, Terashima M, Yang PC, McConnell MV, Nishimura DG, Dai H (2006) FeCo/graphitic-shell nanocrystals as advanced magnetic-resonance-imaging and near-infrared agents. Nat Mater 5:971
93. Huang J, Zhong X, Wang L, Yang L, Mao H (2012) Improving the magnetic resonance imaging contrast and detection methods with engineered magnetic nanoparticles. Theranostics 2(1):86
94. Jang JT, Nah H, Lee JH, Moon SH, Kim MG, Cheon J (2009) Critical enhancements of MRI contrast and hyperthermic effects by dopant-controlled magnetic nanoparticles. Angew Chem Int Ed 48:1234
95. Jun YW, Huh YM, Choi JS, Lee JH, Song HT, Kim S, Yoon S, Kim KS, Shin JS, Suh JS, Cheon J (2005) Nanoscale size effect of magnetic nanocrystals and their utilization for cancer diagnosis via magnetic resonance imaging. J Am Chem Soc 127:5732
96. Ai H, Flask C, Weinberg B, Shuai X, Pagel MD, Farrell D, Duerk J, Gao JM (2005) Magnetite-loaded polymeric micelles as ultrasensitive magnetic-resonance probes. Adv Mater 17:1949
97. Berret J-F, Schonbeck N, Gazeau F, El Kharrat D, Sandre O, Vacher A, Airiau M (2006) Controlled clustering of superparamagnetic nanoparticles using block copolymers: design of new contrast agents for magnetic resonance imaging. J Am Chem Soc 128:1755
98. Na HB, Lee JH, An K, Park YI, Park M, Lee IS, Nam D-H, Kim ST, Kim S-H, Kim S-W, Lim K-H, Kim K-S, Kim S-O, Hyeon T (2007) Development of a T1 contrast agent for magnetic resonance imaging using MnO nanoparticles. Angew Chem Int Ed 46(28):5397
99. Shin J, Anisur RM, Ko MK, Im GH, Lee JH, Lee IS (2009) Hollow manganese oxide nanoparticles as multifunctional agents for magnetic resonance imaging and drug delivery. Angew Chem Int Ed 48:321
100. Duan H, Kuang M, Wang X, Wang YA, Mao H, Nie S (2008) Reexamining the effects of particle size and surface chemistry on the magnetic properties of iron oxide nanocrystals: new insights into spin disorder and proton relaxivity. J Phys Chem C 112:8127
101. Tong S, Hou S, Zheng Z, Zhou J, Bao G (2010) Coating optimization of superparamagnetic iron oxide nanoparticles for high T2 relaxivity. Nano Lett 10:4607
102. Koenig SH, Kellar KE (1995) Theory of 1/T1 and 1/T2 NMRD profiles of solutions of magnetic nanoparticles. Magn Reson Med 34:227
103. Weissleder R, Moore A, Mahmood U, Bhorade R, Benveniste H, Chiocca E, Basilion JP (2000) In vivo magnetic resonance imaging of transgene expression. Nat Med 6:351
104. Jun YW, Lee JH, Cheon J (2008) Chemical design of nanoparticle probes for high-performance magnetic resonance imaging. Angew Chem Int Ed 47:5122
105. Bulte JWM, Douglas T, Witwer B, Zhang SC, Strable E, Lewis BK, Zywicke H, Miller B, van Gelderen P, Moskowitz BM, Duncan ID, Frank JA (2001) Magnetodendrimers allow endosomal magnetic labeling and in vivo tracking of stem cells. Nat Biotechnol 19:1141
106. de Vries IJM, Lesterhuis WJ, Barentsz JO, Verdijk P, van Krieken JH, Boerman OC, Oyen WJG, Bonenkamp JJ, Boezeman JB, Adema GJ, Bulte JWM, Scheenen TWJ, Punt CJA, Heerschap A, Figdor CG (2005) Magnetic resonance tracking of dendritic cells in melanoma patients for monitoring of cellular therapy. Nat Biotechnol 23:1407
107. Zhao M, Beauregard DA, Loizou L, Davletov B, Brindle KM (2001) Non-invasive detection of apoptosis using magnetic resonance imaging and a targeted contrast agent. Nat Med 7:1241

108. Schellenberger EA, Sosnovik D, Weissleder R, Josephson L (2004) Magneto/optical Annexin V, a multimodal protein. Bioconjugate Chem 15:1062
109. Sosnovik D, Weissleder R (2007) Emerging concepts in molecular MRI. Curr Opin Biotechnol 18:4
110. Harisinghani MG, Barentsz J, Hahn PF, Deserno WM, Tabatabaei S, van de Kaa CH, de la Rosette J, Weissleder R (2003) Noninvasive detection of clinically occult lymph-node metastases in prostate cancer. N Engl J Med 348:2491
111. Kapp DS, Hahn GM, Carlson RW (2000) Principles of hyperthermia. Decker, Ontario
112. Gü S (2004) Nanoparticles: from theory to application. Wiley-VCH, Weinheim
113. Mornet S, Vasseur S, Grasset F, Duguet E (2004) Magnetic nanoparticle design for medical diagnosis and therapy. J Mater Chem 14:2161
114. Andra W, Nowak H (1998) Magnetism in medicine: a handbook. Wiley-VCH, Berlin
115. Hergt R, Andra W, d'Ambly CG, Hilger I, Kaiser WA, Richter U, Schmidt HG (1998) Physical limits of hyperthermia using magnetite fine particles. IEEE Trans Magn 34:3745
116. Fortin JP, Wilhelm C, Servais J, Ménager C, Bacri JC, Gazeau F (2007) Size-sorted anionic iron oxide nanomagnets as colloidal mediators for magnetic hyperthermia. J Am Chem Soc 129:2628
117. Eggeman AS, Majetich SA, Farrell D, Pankhurst QA (2007) Size and concentration effects on high frequency hysteresis of iron oxide nanoparticles. IEEE Trans Magn 43:2451
118. magforce. www.magforce.com
119. Hergt R, Dutz S, Röder M (2008) Effects of size distribution on hysteresis losses of magnetic nanoparticles for hyperthermia. J Phys: Condens Matter 20:385214
120. Rosensweig RE (2002) Heating magnetic fluid with alternating magnetic field. J Magn Magn Mater 252:370
121. Hergt R, Dutz S, Ziesberger M (2010) Validity limits of the Néel relaxation model of magnetic nanoparticles for hyperthermia. Nanotecnology 21:015706
122. Carrey J, Mehdaoui B, Respaud M (2011) Simple models for dynamic hysteresis loop calculations of magnetic single-domain nanoparticles: Application to magnetic hyperthermia optimization. J Appl Phys 109:083921
123. Tefferi A (2003) A contemporary approach to the diagnosis and management of polycythemia vera. Curr Hematol Rep 2(3):237
124. Kuimova MK (2012) Mapping viscosity in cells using molecular rotors. Phys Chem Chem Phys 14(37):12671
125. Wang X, Tang J, Shi L (2010) Induction heating of magnetic fluids for hyperthermia treatment. IEEE Trans Mag 46:1043
126. Zhang LY, Gu HC, Wang XM (2007) Magnetite ferrofluid with high specific absorption rate for application in hyperthermia. J Mag Mag Mater 311:228
127. Wang X, Gu H, Yang Z (2005) The heating effect of magnetic fluids in an alternating magnetic field. J Magn Magn Mater 293:334
128. Fortin JP, Gazeau F, Wilhelm C (2008) Intracellular heating of living cells through Néel relaxation of magnetic nanoparticles. Biophys Lett 37:223
129. Ma M, Wu Y, Zhou J, Sun Y, Zhang Y, Gu N (2004) Size dependence of specific power absorption of Fe_3O_4 particles in AC magnetic field. J Magn Magn Mater 268:33
130. de la Presa P, Luengo Y, Multinger M, Costo R, Morales MP, Rivero G, Hernando A (2012) Study of heating efficiency as a function of concentration, size, and applied field in γ-Fe_2O_3 nanoparticles. J Phys Chem 116:25602
131. Motoyama J, Hakata T, Kato R, Yamashita N, Morino T, Kobayashi T, Honda H (2008) Hyperthermic treatment of DMBA-induced rat mammary cancer using magnetic nanoparticles. Biomagnetic Res Techn 6(4):1
132. Cótica LF, Santos IA, Girotto EM, Ferri EV, Coelho AA (2010) Surface spin disorder effects in magnetite and poly(thiophene)-coated magnetite nanoparticles. J Appl Phys 108:064325
133. Guardia P, Batlle-Brugal B, Roca AG, Iglesias O, Morales MP, Serna CJ, Labarta A, Batlle X (2007) Surfactant effects in magnetite nanoparticles of controlled size. J Magn Magn Mater 316:e756

134. Dionigi C, Piñeiro Y, Riminucci A, Bañobre-López M, Rivas J, Dediu V (2013) Regulating the thermal response of PNIPAM hydrogels by controlling the adsorption of magnetite nanoparticles. Appl Phys A (in press)
135. Regmi R, Bhattarai SR, Sudakar C, Wani CS, Cunningham R, Vaishnava PP, Naik R, Oupicky D, Lawes G (2010) Hyperthermia controlled rapid drug release from thermosensitive magnetic microgels. J Mater Chem 20:6158
136. Urtizberea A, Natividad E, Arizaga A, Castro M, Mediano A (2010) Specific absorption rates and magnetic properties of ferrofluids with interaction effects at low concentrations. J Phys Chem C 114:4916
137. Linh PH, Thach PV, Tuan NA, Thuan NC, Mahn DH, Phuc NX, Hong LV (2009) Magnetic fluid based on Fe_3O_4 nanoparticles: preparation and hyperthermia application. J Phys: Conf Ser 187:012069
138. Martinez-Boubeta C, Simeonidis K, Serantes D, Conde-Leborán I, Kazakis I, Stefanou G, Peña L, Galceran R, Balcells L, Monty C, Baldomir D, Mitrakas M, Angelakeris M (2012) Adjustable hyperthermia response of self-assembled ferromagnetic Fe-MgO core–shell nanoparticles by tuning dipole–dipole interactions. Adv Funct Mater 22(17):1
139. Calvo-Fuentes J, Rivas J, López-Quintela MA (2012) Synthesis of subnanometric metal nanoparticles. In: Bhushan B (ed) Encyclopedia of nanotechnology. Springer Verlag, Heidelberg, Germany, p 2639